DEPARTMENT OF COMMERCE
FREDERICK H. MUELLER, Secretary

WEATHER BUREAU
F. W. REICHELDERFER, Chief

MONTHLY WEATHER REVIEW

JAMES E. CASKEY, JR., Editor

Volume 88
Number 7

JULY 1960

Closed September 15, 1960
Issued October 15, 1960

ANALYSIS OF SOME PRELIMINARY LOW-LEVEL CONSTANT LEVEL BALLOON (TETROON) FLIGHTS [1]

J. K. ANGELL AND D. H. PACK

U.S. Weather Bureau, Washington, D.C.

[Manuscript received June 29, 1960; revised July 19, 1960]

ABSTRACT

An analysis is presented of low-level trajectory data obtained by means of constant level balloon flights from Cape Hatteras, N.C., during September and October 1959. An approximately constant floating level was obtained by flying the nearly constant volume Mylar balloons (tetroons) with an internal superpressure of about 100 mb. The metalized tetroons were positioned at 1-min. intervals by means of a manually operated SP–1M radar. From knowledge of these positions, overlapping 5-min. average velocities were determined for flight durations of up to 5 hr. On some of the flights the radar return was enhanced by the addition of a radar reflective mesh to the tetroon. With the addition of this mesh, flights at altitudes of less than 5,000 ft. were tracked as far as 92 n. mi. from the radar, or approximately to the radar horizon.

Spectral analysis of the velocity data obtained from the four best flights shows some evidence for a (Lagrangian) wind speed periodicity of 26-min. period, a vertical motion periodicity of 13-min. period, and a cross-stream velocity periodicity of 17-min. period. Cross spectrum analysis shows that, with the exception of oscillations of 45-min. period, the wind speed is at a maximum ahead of the trough in the trajectory. Thus, if the large-scale air flow is nearly geostrophic, there is evidence that kinetic energy and momentum are transported down the pressure gradient by these small-scale oscillations. The maximum upward motion of the tetroon tends to take place near the trajectory trough line for oscillations of a period exceeding 18 min. and near the trajectory crest for oscillations of smaller period. Therefore, looking downstream, the longer-period tetroon oscillations tend to be counterclockwise in a plane normal to the mean trajectory while the shorter-period oscillations tend to be clockwise. However, until more information is obtained on the small-scale temperature field and the extent to which the tetroons follow the vertical air motion, any statement regarding "direct" and "indirect" air circulations is tentative.

The ratio of one minus the cross-stream and one minus the along-stream autocorrelation coefficients for these flights is approximately 0.6, suggesting a certain similarity between Eulerian space and Lagrangian autocorrelation coefficients. The tetroon data also indicate that initially one minus the cross-stream autocorrelation coefficient is proportional to the time, as would be anticipated from Lagrangian turbulence theory. These data tend to confirm that, for the scale of motion under consideration, the Lagrangian-Eulerian scale factor β of Hay and Pasquill has a value near 4.

1. INTRODUCTION

Constant level balloons offer a means for approximating the trajectory of an air parcel in space. The transosonde program of the United States Navy has demonstrated the usefulness of such balloons for the delineation of the large-scale air flow at jet stream levels over a large segment of the Northern Hemisphere [1, 2]. The purpose of this article is to show how constant level balloons may be utilized for the delineation of the small-scale air flow at levels near the surface and at distances up to 100 n. mi. from a radar site. The Lagrangian fluctuations derived

[1] Work performed in connection with Weather Bureau research for the U.S. Atomic Energy Commission and the U.S. Public Health Service.

from such low-level flights are of great interest in turbulence and diffusion studies.

2. THE SUPERPRESSURED BALLOON CONCEPT

Previous attempts to obtain the Lagrangian characteristics of the air flow at low levels have, in most cases, been based on the use of "neutral" or "no-lift" elastic balloons. While information of interest has been obtained from such flights [7], they have not proved particularly suitable for the determination of the Lagrangian characteristics of the flow over relatively long distances. Since constant volume, superpressured balloons have the capability of floating along a constant density surface almost indefinitely (barring large vertical air motions), it is appropriate to consider their use for this problem.

A balloon ascends or descends in the atmosphere according to whether its bouyancy force, $V_b(\rho_a-\rho_h)$, (where V_b is balloon volume, ρ_a is air density, and ρ_h is the density of a gas lighter than air, in this instance, helium) exceeds or is less than the weight, W_b, of the balloon system. However, if the balloon is of constant volume then, for a given mass of helium introduced into the balloon at the earth's surface, there is a certain air density where the bouyancy force and the weight of the balloon system balance. The 3-dimensional surface along which the atmosphere possesses this density is the surface along which the constant volume balloon will float. The balloon will continue to float along this surface as long as it remains at full volume. The balloon may go slack owing to seepage of helium through the skin of the balloon, through nighttime cooling of the balloon and inclosed helium due to radiation fluxes, or through cooling of the balloon due to any other causes. For these reasons it is desirable that initially, at flight level, the helium within the balloon exert a greater pressure than that of the ambient air. This pressure excess is known as superpressure. Analytically, the helium pressure (p_h) required to prevent a slack balloon at the cold temperature T_c is given by

$$p_h=(T_w/T_c)p_a \tag{1}$$

where p_a is the ambient air pressure and T_w is the warm temperature. For example, if one assumes that a constant volume balloon flying at 900 mb. possesses a temperature of 300° A. during the day and a temperature of 280° A. during the night, then a daytime superpressure of 63 mb. would suffice to keep the balloon fully inflated at night. While statistics on day-night balloon temperatures at low flight levels are not yet available, one would expect that a daytime superpressure of 100 mb. would be suffiicient to carry the balloon through the nighttime hours with no deviation from the density surface.

3. EQUIPMENT AND FLIGHT TECHNIQUES

A relatively new polyester film called Mylar [2] is highly suitable for use in the construction of constant volume balloons since it possesses very low permeability and high tensile strength (13,000 lb. in.$^{-2}$). It can be shown that a spherical Mylar balloon of 1-foot radius and a skin thickness of only 2 mils (2/1000 in.) is capable of supporting a superpressure of 150 mb., thus undoubtedly satisfying the day-night requirements mentioned above. Furthermore, while it was originally feared that the seals or gores on the balloon would be unable to withstand such a superpressure, it was found that the G. T. Schjeldahl Company of Northfield, Minn. had perfected a method of heat sealing which yielded a seal strength comparable to that of the Mylar itself. For purposes of economy and reliability, however, it was desirable that these seals be straight lines. Therefore, tetrahedron-shaped balloons rather than spherical balloons were constructed for our experiments. Combination of the word "tetrahedron" and the word "balloon" results in the word "tetroon" as a designator for these particular balloons.

Tetroons with a side length of 36, 42, and 60 in. (nominal volumes, respectively, of 0.20, 0.32, 0.94 m.^{3}) have been used in our experiments. It is desirable that the tetroon volume not exceed about 3 m.^{3} partially in order to comply with regulations of the Federal Aviation Agency concerning the flying of balloons within air space. With no weight attached, the ceiling of the 42-in. tetroon is about 10,000 ft. while the ceiling of the 60-in. tetroon is about 20,000 ft. Figure 1 shows a picture of a 42-in. tetroon with inflation rig and manometer (for measuring superpressure) attached. Note that the tetroon has been coated with a molecular film of aluminum in order to provide a radar target.

Some of the earlier tetroon flights suggested that the tetroon volume was not being conserved under conditions of considerable superpressure, since the tetroons were flying at a higher elevation than would be anticipated from the balance of bouyancy force and weight on the assumption of constant balloon volume. If the tetroon volume is not absolutely constant as it ascends through the atmosphere it can be seen, by equating the weight of the balloon system and the bouyancy force, that the weight, X, which must be attached to the tetroon to enable it to fly at a given density surface is

$$X=V_e(\rho_a-\rho_h)-W_b=V_e\rho_a-V_s\rho_{hs}-W_b \tag{2}$$

where V_s is the tetroon volume at the earth's surface, $V_e=V_s+\Delta V$ is the tetroon volume at flight level, ρ_a is the air density at flight level, ρ_h is the helium density at flight level, ρ_{hs} is the helium density at the earth's surface, and W_b is the weight of the balloon system.

Differentiating equation (2) with respect to pressure it is found that

$$\frac{\delta X}{\delta p}=V_e\frac{\delta \rho_a}{\delta p}+\rho_a\frac{\delta V_e}{\delta p}. \tag{3}$$

The right hand term in this equation is negative since

[2] Mylar—a trade name for a polyester film manufactured by the E. I. du Pont Company of Wilmington, Del.

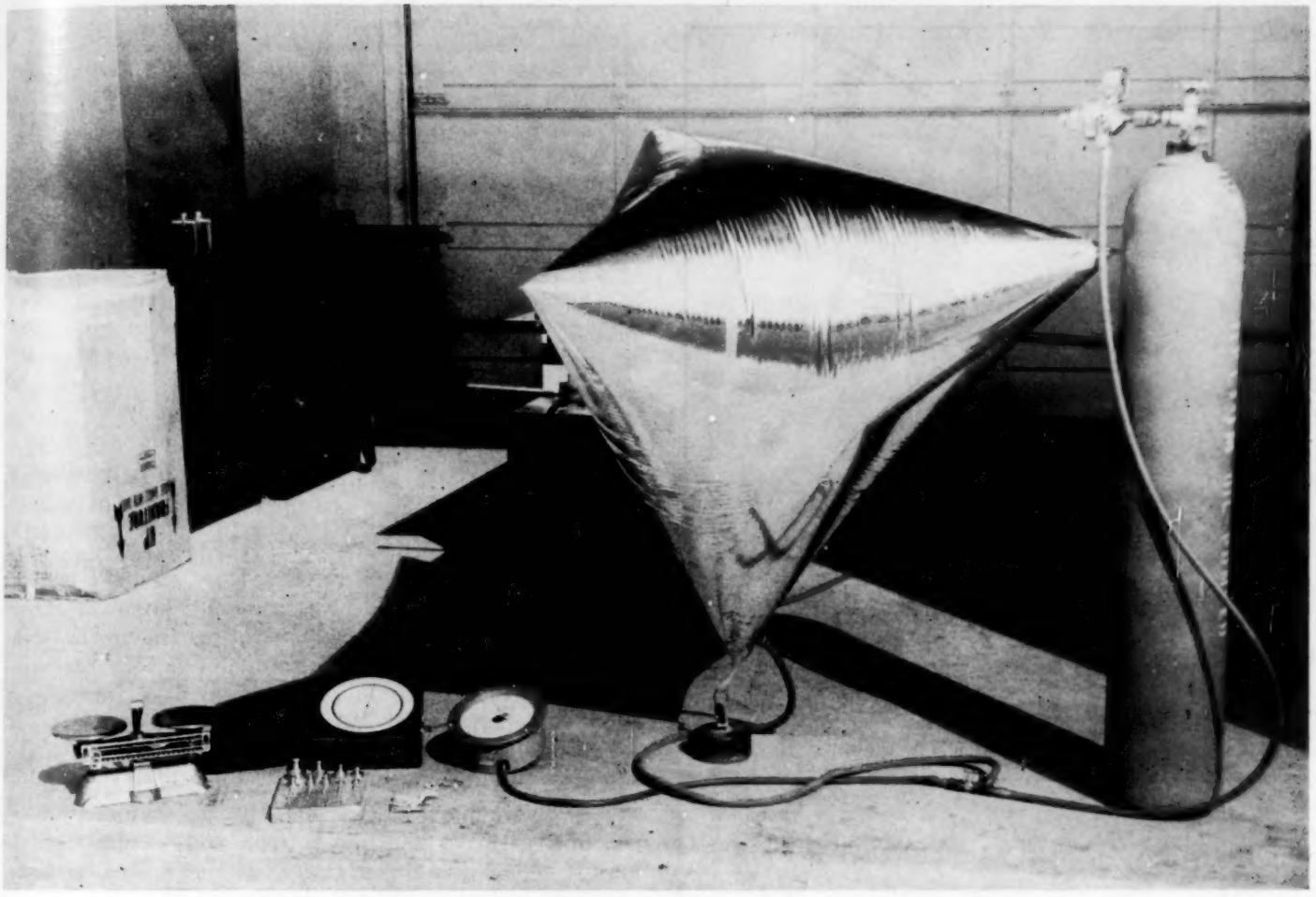

FIGURE 1.—Photograph of 42-in. tetroon with inflation rig and manometer attached.

tetroon volume increases with decrease in ambient pressure (increase in superpressure). If this negative term becomes larger in magnitude than the middle term in equation (3), the equation states that more weight must be attached to the tetroon to make it float at a low pressure (high level) than at a high pressure (low level). Under these conditions the tetroon is not in stable equilibrium at any level but continuously ascends, thus in no sense performing the function of a constant level balloon. This takes place when the volume increase of the tetroon associated with increase in superpressure more than offsets the decrease in bouyancy force brought about by the decrease, with decrease in ambient air pressure, of the density difference between helium and air. It is apparent that the change of tetroon volume with increase in superpressure must be determined precisely, not only to permit the flying of the tetróons at the required altitude, but also to ensure that a constant level balloon flight actually results.

The change in tetroon volume as a function of superpressure was determined by careful weigh-off at the ground. The amount of superpressure within the tetroon was measured by a sensitive manometer while the tetroon volume, V_b, was determined from the equation

$$V_b=\frac{W_b+L}{\rho_{as}-\rho_{hs}} \tag{4}$$

where L is the free lift of the tetroon (measured by sensitive scales), ρ_{as} is surface air density, and the other parameters are as defined previously. Each of the tetroons tested was taken in steps up to a superpressure of 150 mb. with the tetroon volume being determined at each step. The tetroons were then deflated (a vacuum cleaner is suitable, and necessary, for this) to near zero superpressure in order to note whether the volume change persisted. It was found that the tetroons are semi-elastic with about one-half the volume change remaining after deflation to a small superpressure. Figure 2 shows, by small circles, the 42-in. tetroon volume change as a function of superpressure when the tetroons are first brought up to a superpressure of 150 mb. The analytic expression approximately fitting these circles is

$$\Delta V=0.0038(e^{0.015\Delta p}-1) \tag{5}$$

where ΔV is the volume change in cubic meters and Δp

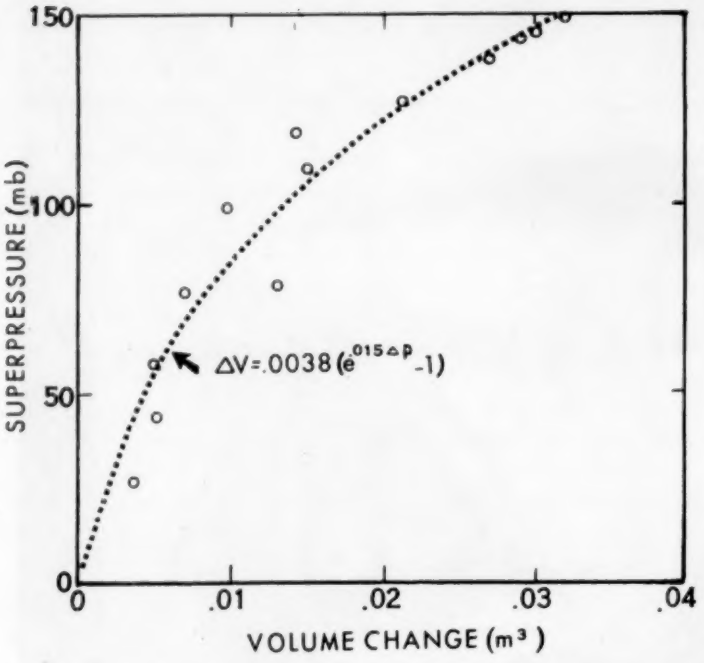

FIGURE 2.—Volume changes of 42-in. tetroons as a function of tetroon superpressure (circles) and the fit of an analytic expression to these values (dotted line).

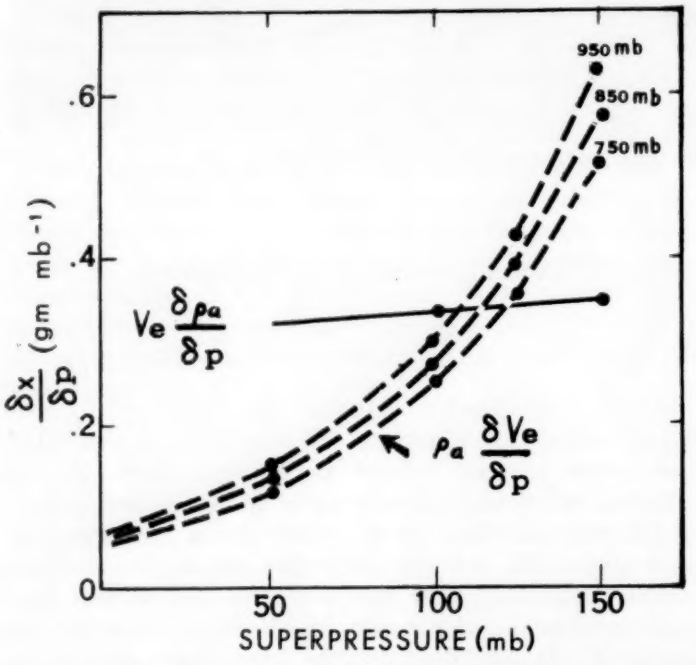

FIGURE 3.—Relative magnitudes of the density-change term (solid line) and the volume-change term for various pressure heights (dashed line) in equation (3) as a function of tetroon superpressure (abscissa). The ordinate gives the change in the weight to be attached to the tetroon to enable it to fly at a different pressure surface Δp millibars away.

is the superpressure in millibars. Of great interest are the conditions under which the volume change of the 42-in. tetroon given by equation (5) is of sufficient magnitude to over-compensate the density-change term in equation (3), since if this criterion is satisfied the tetroon is no longer a constant level balloon. Figure 3 shows the relative magnitudes of the density-change term (solid line) and the volume-change term for various pressure-heights (dashed lines) in equation (3) as a function of tetroon superpressure (abscissa). Since the volume-change term in figure 3 is plotted as the negative of the way it appears in equation (3), it is seen that if the tetroon superpressure much exceeds 100 mb., the ordinate, $\delta X/\delta p$, becomes negative and the tetroon will ascend until it bursts. Consequently, if these tetroons are to be flown at ambient pressures of less than 900 mb., it is necessary to launch them in a partially deflated state. Procedures for determining the weight to be added to the tetroon in order to attain flight at a given density surface are given in the appendix for cases when (a) the tetroon volume is assumed constant, (b) the flight is to be made at low levels and the tetroon volume is assumed to vary according to equation (5), and (c) the tetroon is launched in a semi-deflated state for flight at high level and the tetroon volume is assumed to vary according to equation (5).

TABLE 1.—*Tetroon tracking experiments during 1958-59*

Location	Date	Tracked by	Max. range (n. mi.)	Results
Naval Research Laboratory, Chesapeake Bay Annex.	9-58	Mark 25 (3-cm.), ANA/SPQ-2X1 (10-cm.) fire control radar and optical theodolite.	9	Good.
Oak Ridge, Tenn. (Oak Ridge National Laboratory).	9-58	Decca 40 (3-cm.) Weather radar (fixed antenna).	?	Ambiguous.
Dawsonville, Ga. (Georgia Nuclear Laboratory, Lockheed Aircraft Corp.).	10-58	Decca 40 (3-cm.) Weather radar (fixed antenna).	?	Ambiguous.
Idaho Falls, Idaho (National Reactor Testing Station).	11-58	Modified APS-3 (10-cm.) radar.	4	Poor.
Oak Ridge, Tenn.	3-59	FPS-10 (10-cm.) radar and optical theodolite.	4-6	Poor, no radar return.
Manassas, Va. (U.S. Air Force, Air Defense Command).	3-59	FPS-3 (23-cm.) radar.	(Altitude 5,000 ft.) 15. (Altitude 10,000 ft.) 60.	Fair. Good.
Hatteras, N.C. (U.S. Weather Bureau station).	9-59 to 10-59	Modified SP-1M (10-cm.) radar.	92	Excellent.

4. SUMMARY OF TETROON FLIGHTS DURING 1958-59

Table 1 gives a summary of tetroon flights made through the year 1959. Tetroon flights were first made at the Chesapeake Bay Annex of the Naval Research Laboratory, where the attachment of a metalized mesh to the aluminized tetroon permitted the balloon to be tracked for 9 mi. Without this mesh the radar returns were sporadic, probably depending upon whether the face or the corner of the tetroon was directed toward the radar. Figure 4 shows three altitude-versus-time plots of the most successful tetroon flight at the Chesapeake Bay Annex, as obtained from radar information and a combination of radar and visual theodolite information. Of interest in this figure is the evidence that the tetroon overshot its floating level and subsequently performed damped vertical oscillations of a period (in this case) of about 20 min.

Later tetroon flights at Oak Ridge, Tenn. and Dawsonville, Ga. were not successful. Conditions for tracking were poor with precipitation echoes scattered over the Decca PPI scope. In addition, the ground clutter was bothersome at both stations. Poor results also were obtained from the tetroon flights made at Idaho Falls, Idaho, in November 1958, probably owing to the low power of the modified APS–3 radar.

The Air Defense Command (ADC) radar at Oak Ridge was unsuccessful in attempting to track tetroons in March 1959. Again precipitation was present in the vicinity of the radar and it is believed that at least one tetroon entered a region of precipitation and was forced to the ground. On the other hand, tetroon flights made from the U.S. Air Force ADC site at Manassas, Va. during this same month were moderately successful, and sporadic tracking of a 10,000-ft. flight was carried out for a distance of 60 mi. A longer track might have been obtained except for the fact that the constant level tetroons tend to fly out of the cone of vision of the upward-directed ADC radars. The long strips of aluminized Mylar suspended from the tetroon corners on some of the Manassas flights did not noticeably improve the radar reflectivity of the balloon system and proved most unwieldly during launching.

Finally, in September and October 1959, tetroon flights were made from the Weather Bureau Station at Cape Hatteras, N.C. Tracking was accomplished by means of the manually operated SP–1M radar of the Weather Bureau. These flights were most successful, and consequently, the remainder of this article is devoted to these flights and the meteorological results obtained therefrom.

5. TETROON FLIGHTS FROM CAPE HATTERAS

A. EQUIPMENT AND PROCEDURES

The SP–1M radar at Cape Hatteras has a power of 750 kw., a wavelength of 10 cm., and a conical beam width of 3.4°. The range accuracy of the SP–1M is stated only as being within 200 yd. If it is assumed that this means that 99 percent of the time the error in range is less than 200 yd., then assuming a Gaussian distribution of range errors, the average range error would be 77 yd. Since the error in the difference between two quantities equals the square root of the sum of the squares of the individual errors, the average error in distance between two radar-determined ranges would be 109 yd. Thus it is estimated that the average SP–1M-determined tetroon speed error, ΔV, in knots, for a tetroon moving radially away from the radar would be given by

$$\Delta V = 3.2/T \qquad (6)$$

where T is the time interval between positions in minutes. One might like to make T large in order that the error in tetroon speed determination be small. On the other hand, the larger T is chosen, the more the high frequency speed oscillations are damped. The compromise adopted here involved the determination of speed over a 5-min. interval, thus presumably yielding an average speed error of 0.64 kt. and introducing a 50 percent reduction in the magnitude of oscillations of 8-min. period. Figure 5 shows by means of solid lines this theoretical error in wind speed and, for comparison, the regression line of the observed average absolute deviation of tetroon speed from the 20-min. average value as a function of radar range. Since there is no reason to expect the actual speed oscillations to increase in magnitude with distance from the

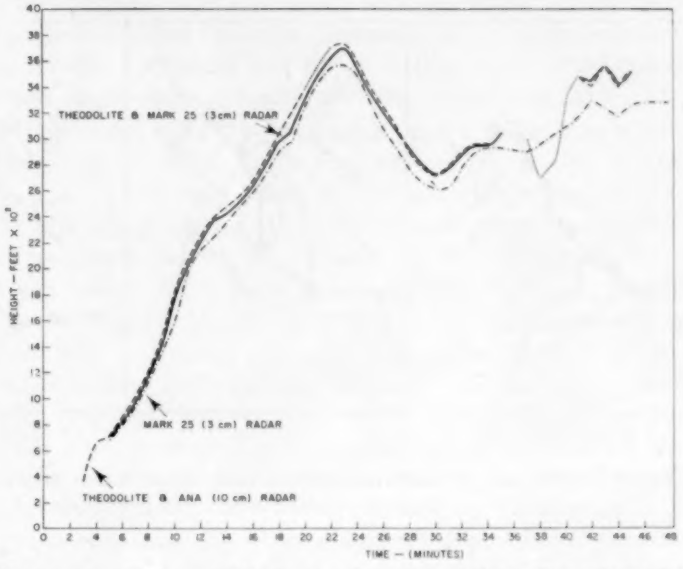

FIGURE 4.—Tetroon altitude as a function of time after release for Flight 2 from the Chesapeake Bay Annex.

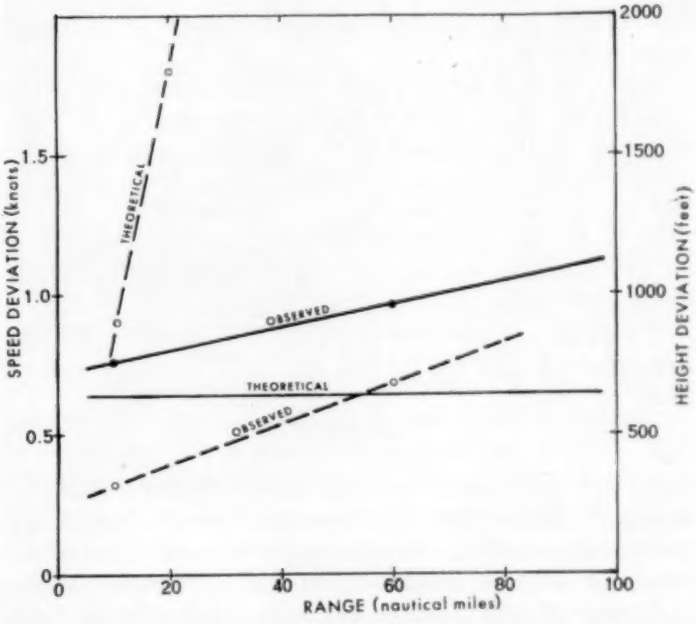

FIGURE 5.—Theoretical average errors in tetroon speed (solid line) and height (dashed line) as a function of range for the SP–1M radar at Hatteras. The remaining pair of lines gives the observed average absolute deviation of speed and height from 20-min. average values as a function of range for the tetroon flights from Cape Hatteras.

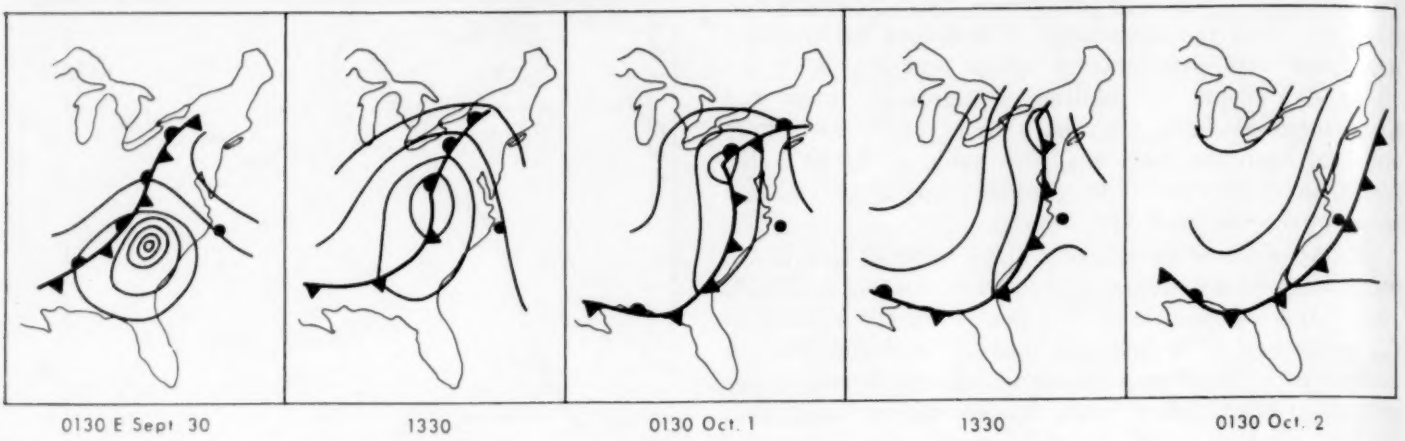

FIGURE 6.—Surface pressure patterns at 12-hr. intervals during the period of tetroon flights from Cape Hatteras. The position of the Cape Hatteras Station is indicated by the heavy dot. Isobars drawn at 4-mb. intervals.

radar, the deviation of the observed line from the horizontal probably indicates that actually there is a greater uncertainty in the wind speed determinations as the radar range increases.

Large errors in azimuth and elevation angles may result from the use of the SP–1M radar because of the 3.4° conical beam width (defined as the angular measure of the distance from the power P at the center of beam to 0.5 P) and the lack of a precision target indicator (PTI).

If, in the absence of the PTI, it is assumed that it is equally probable the tetroon will be positioned anywhere within the beam the maximum angular error would be 1.7° with an average error of 0.85°. The average SP–1M-determined height (or lateral) error ΔH, in feet, would be given by

$$\Delta H = 90R \tag{7}$$

where R is the range in nautical miles. Figure 5 shows by means of dashed lines this theoretical error in height determination and, for comparison, the regression line of the observed average absolute deviation of tetroon height from the 20-min. average value as a function of radar range. The observed deviation increases much more slowly than the theoretical, presumably because of the necessity for aligning the target more nearly in the center of the radar beam in order to get a good signal return at great ranges and the subjective tendency not to vary the elevation angle of the radar at these ranges unless forced to do so. The tetroon targets were manually tracked, with one man operating elevation and azimuth controls and one on the range scope. The balloon position was read from these dials at 1-minute intervals. In any event, it is obvious that the vertical and cross-stream motions of the tetroon obtained from the SP–1M radar should be treated with caution.

One of the purposes of the Cape Hatteras tetroon flights was to test the improvement in radar return resulting from use of a metalized nylon mesh obtained from Suchy Division, Inc. of New York. This mesh was formed into a cylinder and hung like a skirt from the mid-section of the tetroon. The mesh weighed only 50 gm. and provided an additional radar-reflecting area of 30 ft.^{2}. Furthermore, the mesh skirt, hanging in the form of a cylinder, greatly lessened the problem of signal fading associated with the shape of the tetroon. The success of the mesh can be judged from the fact that the two tetroons on which it was installed were tracked over the radar horizon.

TABLE 2.—*Tetroon flights from Cape Hatteras, N. C.*

Flight no.	Time of launching (EST)	Date	Flight duration (hr.)	Max. range (n.mi.)	Average height (100's of ft.)	σ_h (100's of ft.)	Average speed (kt.)	σ_v (kt.)	Flight equipment
1	1108	9–30–59	1.7	52	11	(*)	30.6	(*)	42-in. tetroon.
2	1422	9–30–59	4.0	92	42	22	23.0	3.3	42-in. tetroon with 10-cm. radar mesh.
3	2037	9–30–59	1.9	50	16	8	26.3	2.7	60-in. tetroon with 3-cm. radar mesh.
4	0825	10–1–59	4.4	60	40	16	13.6	1.7	Train of 3 42-in. tetroons.
5	1413	10–1–59	5.0	51	143	22	10.2	2.3	60-in. tetroon.

*Not computed—tracking sporadic.
σ_h=Standard deviation of height.
σ_v=Standard deviation of speed.

B. TETROON TRAJECTORIES

Figure 6 shows the surface pressure pattern at 12-hr. intervals during the period of tetroon launchings from Cape Hatteras. The flights were made (inadvertently) while hurricane Gracie was in the process of being transformed into an extratropical storm over the Middle Atlantic States. Consequently, at least 5 min. tracking time was lost each hour due to use of the radar for synoptic observations. Table 2 gives information on the five successful tetroon flights made during this period. From comparison of the tetroon release time, as presented in the table, and the synoptic maps one can visualize the synoptic situation during the tetroon flight. It is seen

from table 2 that in addition to tetroons with metalized mesh attached, tracking was also performed on a plain 42-in. tetroon, a plain 60-in. tetroon, and on three 42-in. tetroons tied together.

Figure 7 shows the trajectories of the five flights. The tetroon positions are plotted at 10-min. intervals while the tetroon velocity, determined from the distance and direction between successive positions, is indicated in conventional meteorological form (in knots). The numbers beneath the positions indicate the tetroon height to the nearest 1,000 ft. All flights except Flight 5 were ballasted to float at 900 mb. (about 3,000 ft.), while Flight 5 was ballasted to float at 700 mb. (about 10,000 ft.). The error in altitude determination of Flight 5 resulted from the assumption that equation (5) applied to 60-in. tetroons as well as to 42-in. tetroons for which it was derived. It is noted that near the end of the trajectories on Flights 2 and 4 there was a sudden jump in the tetroon height as indicated by the radar. Since it is most unlikely that the tetroons appreciably changed altitude, it is probable that these height jumps depict the complex refraction and reflection phenomena of the radar beam near the radar horizon. Therefore, while the horizontal trajectory of the tetroon may be determined near to and even beyond the radar horizon, it is probable that the vertical positions of the tetroon indicated by the radar near the radar horizon are of little significance. If, however, the variations in signal are random, spectral analysis can separate significant vertical motions. Even if the signal variations are ordered there is the possibility, by comparison with data closer to the radar, of identifying the spurious variations due to anomalous propagation.

C. VELOCITY FLUCTUATIONS

Figure 8 shows the speed as a function of time as obtained from the four accurately positioned tetroon flights. This speed was determined only from the change in radar range apropos the discussion in 5a concerning the inaccuracy of azimuth angles determined by the SP–1M radar. The dashed speed traces indicate places where the tetroon speed had to be interpolated, either due to use of the radar for synoptic purposes or to loss of contact with the tetroon through a fading radar signal. The vertical arrows near the beginning of each trace indicate the approximate time the tetroons reached flight altitude. Most apparent in figure 8 is the long term increase of wind speed with time on Flights 2 and 3. A glance at the first 1330 EST map in figure 6 shows that this speed increase is in agreement with the increase of surface pressure gradient as one moves north of Cape Hatteras. On Flight 5 there was a most surprising periodicity in wind speed near the beginning of the flight. Several times the wind speed changed by 6 kt. in about 13 min. of time (2.8 n. mi. travel distance) with some evidence that the speed increase was more abrupt than the speed decrease. More will be said about this periodicity later. The significance of the speed changes shown in figure 8 can be estimated from the discussion of the range accuracy of the SP–1M radar and the deviation of the wind speed from the 20-min. averages presented in section 5a.

For each of the four well-positioned tetroon flights, the contribution of oscillations of various frequency to the variance of the series was determined for the wind speed, V, the along-stream, V_s, and cross-stream, V_n, velocity components (where the "stream" is defined by the total wind vector for a run) and the vertical motion, W, in the manner indicated by Tukey [14]. Spectra were determined separately for both the earlier portion of the flight, when little interpolation of the velocity values was required, and for the entire flight. These spectra were then averaged so that the "good" portion of the flight was weighted twice as heavily as the "poor" portion of the flight. While considering the spectral and autocorrelation curves so obtained it should be kept in mind that the "predominant" periodicities which result are to some extent related to the interval and length of sampling, and furthermore that the fraction of the energy of the velocity represented by V_s and V_n at a given frequency is in part a function of the orientation of the coordinate axes. The degree to which these factors bias the results presented herein will be more readily apparent upon analysis of the precise trajectory data obtained by means of tetroon flights from the Wallops Island station of the National Aeronautics and Space Administration.

The variation with frequency of the speed variance for the individual flights, as well as the mean variance for all the flights, is indicated in the top diagram of figure 9 for periods of oscillation varying from 3 hr. to 6 min. The greatest speed variance is associated with the low frequency oscillations, which are probably "synoptic" or inertial in character. Flights 5 and 3 yield a pronounced tendency for speed fluctuations of period near 26 min. These two flights have sufficient influence on the mean to make the next most pronounced mean periodicity one of 26-min. period. Less pronounced peaks in the mean spectra occur at periods of 12–13 min. and 8 min. Since the speed has been averaged over a 5-min. interval, the spectral peak at 12–13 min. might be due to errors in range determination.

The variation with frequency of the variance of the vertical tetroon motion is given in the lower diagram of figure 9. With the exception of minor peaks of dubious significance, the mean variance of tetroon vertical motion is at a maximum near a period of 13 min. The three possibilities with regard to this peak are: (a) the 13-min. period in tetroon oscillation represents a similar period in vertical air motions, (b) the 13-min. period reflects only vertical tetroon oscillations and does not reflect the vertical air motions at all, and (c) the 13-min. period does not even represent the predominant period of tetroon oscillations but is indicative only of errors in the elevation angles obtained from the SP–1M radar (see section 5a.).

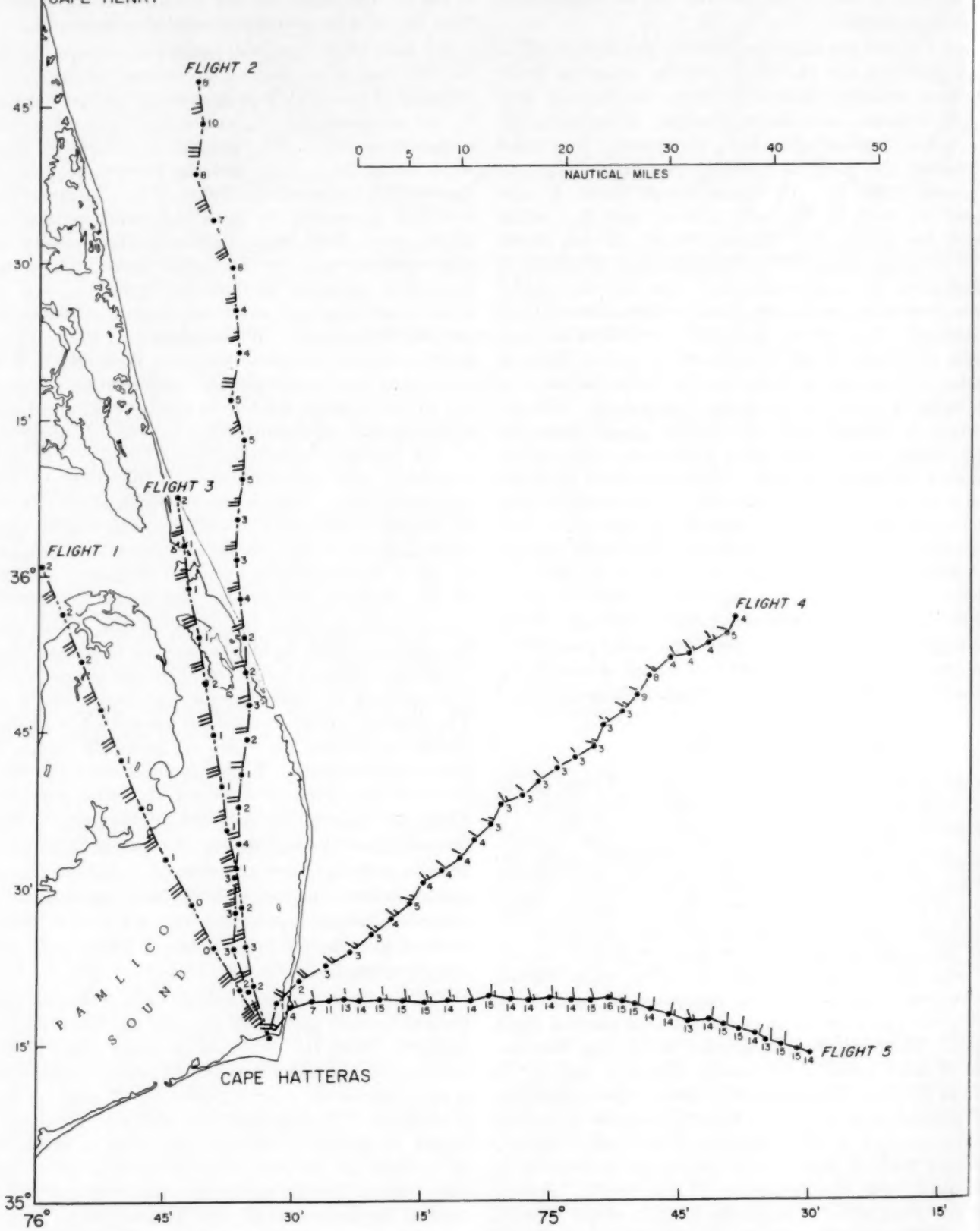

FIGURE 7.—Trajectories of the five tetroon flights from Cape Hatteras. The tetroon positions are plotted at 10-min. intervals, while the tetroon velocity (in knots) is indicated in the conventional meteorological form. The tetroon height in thousands of feet is indicated beneath each position.

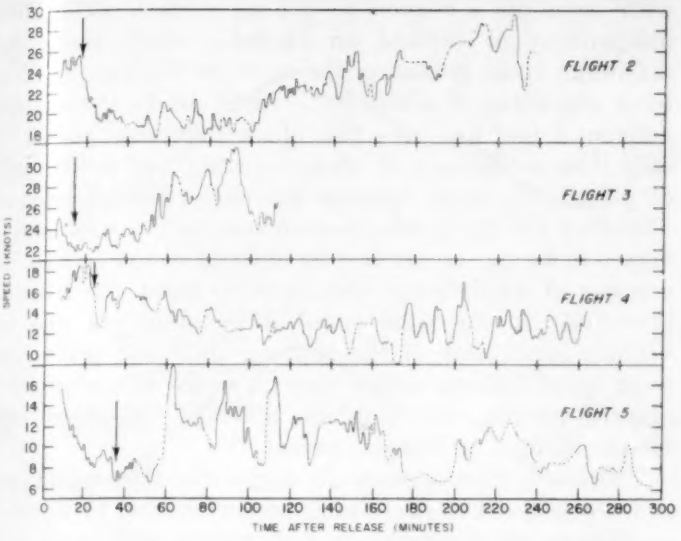

FIGURE 8.—Wind speed as a function of time after release as obtained from the four accurately positioned tetroon flights from Cape Hatteras. The dashed traces indicate interpolated speed values. The arrows indicate the approximate time the tetroons reached flight altitude.

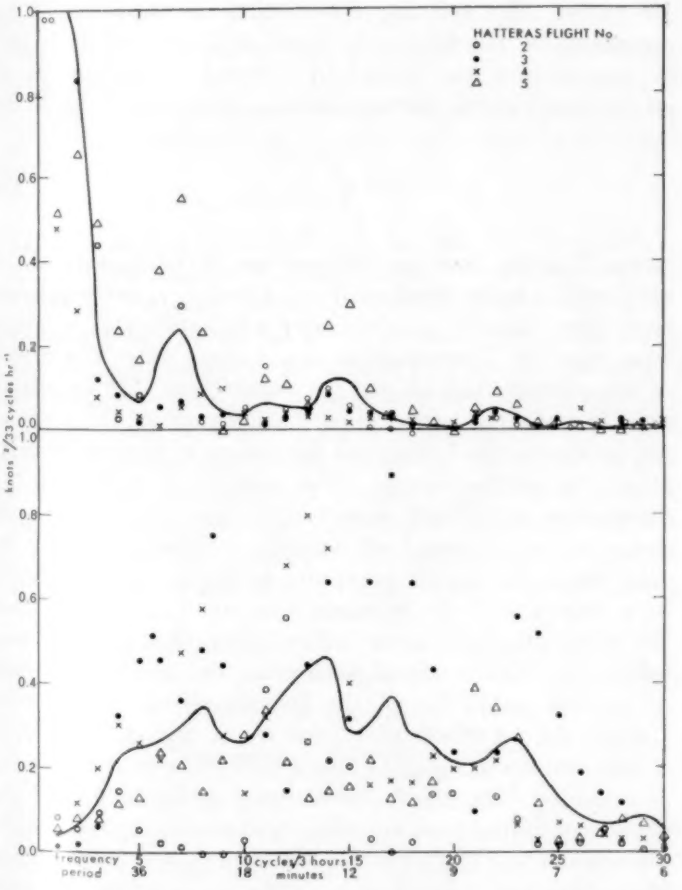

FIGURE 9.—Speed variance (top) and vertical velocity variance (bottom) as functions of frequency of oscillation for individual tetroon flights and the mean of all flights (solid line) from Cape Hatteras.

562159—60——2

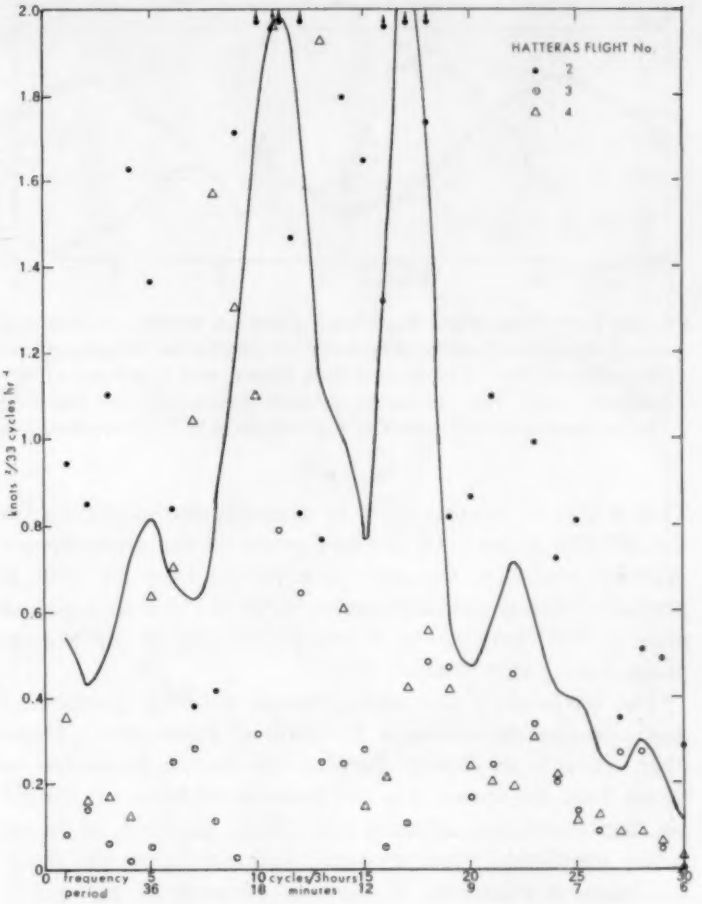

FIGURE 10.—Cross-stream velocity variance as a function of frequency of oscillation for individual tetroon flights and the mean of all flights (solid line) from Cape Hatteras.

Discussion of these possibilities is reserved for the next subsection. It is interesting to note, however, that excluding the variance associated with oscillations of more than a 1-hr. period the flights with relatively large values of the speed variance have relatively small values of the vertical motion variance. Thus Flights 3 and 5 each have a relatively large speed variance (1.9, 4.1 kt.^{2}) and relatively small vertical velocity variance (2.7, 2.8 kt.^{2}) while Flights 2 and 4 each have a relatively small speed variance (1.0, 0.7 kt.^{2}) and a relatively large vertical velocity variance (10.0, 6.8 kt.^{2}). In considering these values it should be remembered that Flight 3 was an evening flight, while Flight 5 was a flight at 14,000 ft. In any event, this negative correlation between the magnitudes of speed and vertical velocity variances suggests that most of the speed variance is not due to vertical oscillations of the tetroons in regions of vertical wind shear.

Figure 10 shows the variance of the cross-stream velocity component as a function of frequency. Note that at all frequencies the variance of the cross-stream velocity component is very large compared to that of the speed.

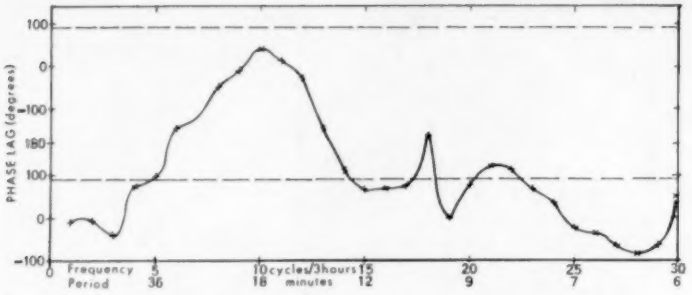

FIGURE 11.—Mean phase lag between tetroon vertical motion and speed as a function of frequency of oscillation for the Cape Hatteras flights. The dashed lines drawn at a phase lag of 90° indicate where the maximum upward tetroon motion followed the maximum tetroon speed by a phase lag of 90° (¼ wavelength).

This is due to uncertainties in azimuth determination by the SP–1M radar. Of the two peaks in the cross-stream velocity variance, the one at a period near 10 min. is probably due to azimuth errors while the one at a period near 17 min. may reflect a real periodicity in the atmosphere during this time.

The variance of the along-stream velocity component was also determined as a function of frequency. However, since it so closely mirrors the results presented in figure 9 for the speed, it is not reproduced here. It should be mentioned that Mantis [13], from analysis of accurately positioned superpressured balloon flights at 30,000 ft., found a minimum of velocity variance at periods of 12–24 min., certainly not in agreement with the results found here.

D. CONSIDERATIONS OF TETROON MOTIONS AS INDICATORS OF AIR MOTIONS

In estimating the degree to which oscillations in the tetroon velocity represent oscillations in air velocity, it is desirable to have knowledge of the phase lag between the oscillations of various velocity components. This phase lag as a function of frequency of oscillation may be obtained from evaluations of the co-variance and quadrature variance in the manner indicated by Van der Hoven and Panofsky [16].

Let us first consider the significance of the speed periodicities indicated by the upper diagram of figure 9. It is apparent that if the tetroon does not follow the vertical air motion but instead, perhaps due to overshooting its flight level initially (fig. 4), undergoes vertical oscillations independent of vertical air motions in a region of vertical wind shear, then a fictitious periodicity in wind speed will be introduced. We should therefore be suspicious of any wind speed periodicity which is associated with a periodicity in vertical tetroon motion. From figure 9 this association is most obvious for oscillations of 12–13-min. period. For further evidence we turn to the phase lag between wind speed and vertical tetroon motion (fig. 11). Since, for all four of the tetroon flights under consideration, the wind speed was decreasing with elevation, a tetroon performing vertical oscillations independent of vertical air motions would show the maximum speed preceding the maximum upward motion by a phase lag of about 90°. In figure 11 the dashed horizontal line indicates this phase difference and it is seen that oscillations of 40-min. period and oscillations of period 13–8 min. possess this 90° phase difference. Therefore the 12–13-min. periodicities in the wind speed may well be due to vertical oscillations of the tetroon in a region of wind shear. On the other hand, the 26-min. periodicity in the wind speed is certainly not due to vertical oscillations of the tetroon, since the maximum wind speed follows rather than precedes the maximum upward motion with a phase difference of about 90° for oscillations of 26-min. period.

The above discussion, while suggesting that variations in tetroon speed of 12–13-min. period are due to vertical oscillations of the tetroons with this period, does not prove that the vertical oscillations were tetroon oscillations only and not those of the air, since a tetroon enclosed in a blob of air would also experience, although to a lesser extent, the component phase lags mentioned above. Therefore, we next determine whether the predominant period of vertical tetroon oscillation is reasonably close to the period which would be expected of an air parcel. By relating the vertical acceleration of an air parcel to the bouyancy force acting upon it, it can be shown that the period of vertical oscillation (τ) of an air parcel in the atmosphere is approximately given by

$$\tau=2\pi\sqrt{\frac{T_0}{g(\gamma_p-\gamma)}} \tag{8}$$

where T_0 is the absolute temperature in the vicinity of the air parcel, g is the acceleration of gravity, γ_p is the process lapse rate (usually assumed dry adiabatic) and γ is the lapse rate [9]. This equation is not exact, since the effects of the surrounding air are not considered. These effects tend to make the period of oscillation greater, the more so the greater is the horizontal dimension of the cell in relation to its vertical extent. For example, in cells with the dimensions of Bénard cells (cell height three times cell diameter), the period of vertical oscillation would be 1.46 times the period given by equation (8) [5]. Since it is impractical to estimate the cell dimensions from the tetroon flights it must suffice to say, that if the tetroon follows the 3-dimensional path of an air parcel, the period of vertical oscillation of the tetroon should be between τ and 1.5τ. Table 3 gives, for the 4 flights, the period of maximum variance of tetroon oscillation in the vertical, as obtained from the lower diagram of figure 9, and the period computed from equation (8) by utilizing radiosonde ascents at Cape Hatteras to yield information on the mean lapse rates and temperatures at the average floating level of the tetroons. In all cases the predominant periodicity in tetroon oscillation in the vertical exceeded that given by equation (8), with the multiplication factor being 1.1 on

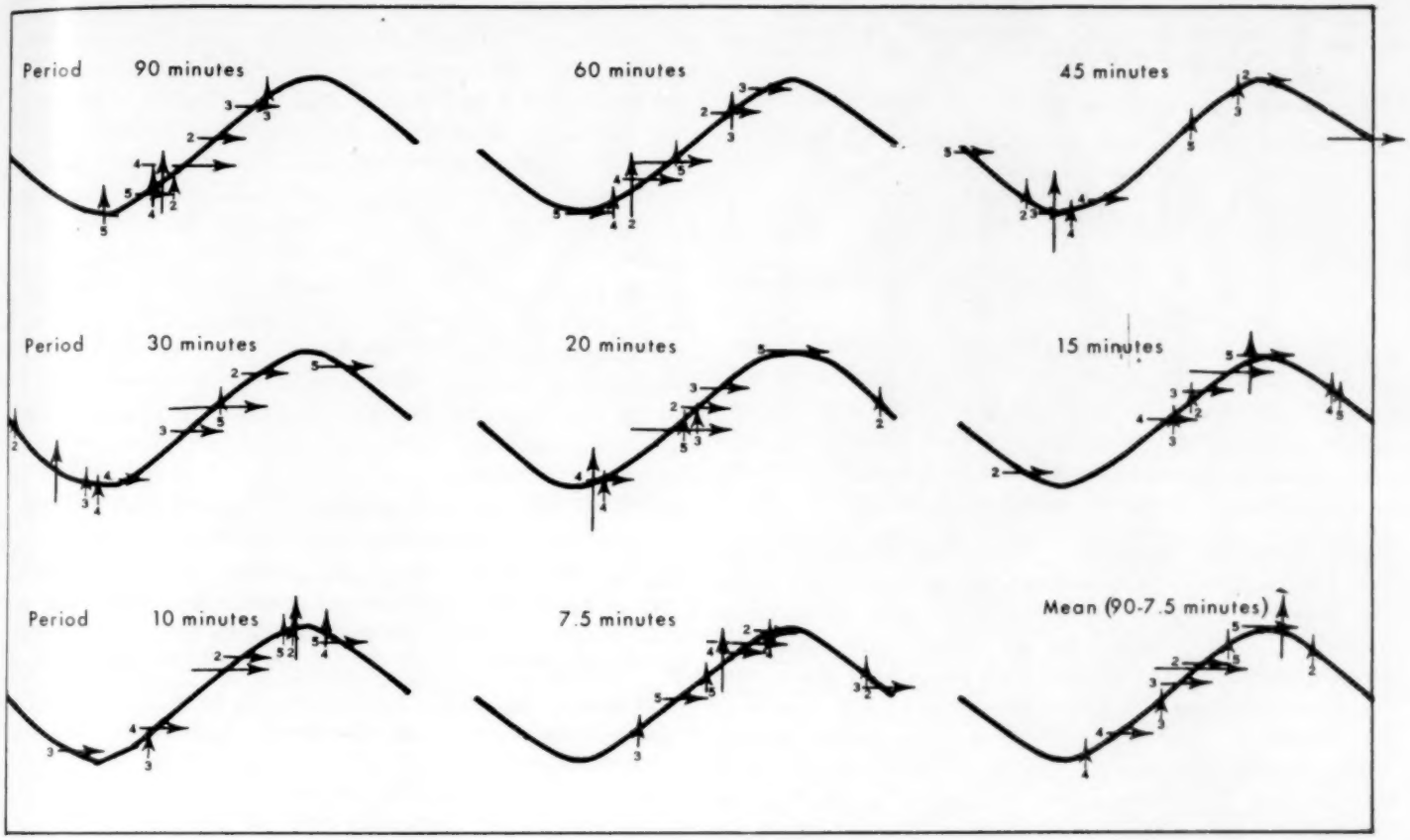

FIGURE 12.—Positions of maximum tetroon speed (horizontal arrows) and maximum tetroon upward motion (vertical arrows) relative to tetroon transversal velocity components (schematic wave-shaped trajectories) for oscillations of various periods (in minutes) for the individual numbered flights and the mean of all flights (long arrows) from Cape Hatteras.

Flights 2 and 5, 1.3 on Flight 3, and 1.8 on Flight 4. On the other hand, the natural period of oscillation of an absolutely constant volume tetroon (neglecting aerodynamic drag which, for the tetrahedrons, must be a complicated (and unknown) non-linear function of the restoring buoyancy force) in an atmosphere with the given stability would be about one-fourth the observed 13-min. period of vertical oscillation, while the period of vertical oscillation of a completely elastic helium-filled balloon (helium lapse rate equals 1.3° C. per 100 m.) would be about one-half the observed predominant period. Thus the predominant period of 13 min. is not due to natural vertical oscillations of the tetroon and the hypothesis that the tetroon at least partially follows the vertical air motion is certainly not contradicted except perhaps in the case of Flight 4. However, since this latter flight consisted of 3 tetroons tied together (which probably had different natural floating levels), it would not be surprising to find vertical air motions poorly represented by the vertical motions of this tetroon train.

TABLE 3.—*Comparison of predominant period of tetroon vertical motion and theoretical period of vertical air motion for Cape Hatteras flights*

Flight	Predominant tetroon period (min.)	Period computed from equation (8) (min.)
2	10.6	9.4
3	15.0	11.2
4	13.8	7.7
5	8.6	8.0

E. PHASE LAG BETWEEN CROSS-STREAM FLOW, AND MAXIMUM SPEED AND UPWARD MOTION FOR OSCILLATIONS OF DIFFERENT PERIODS

Figure 12 gives the position of maximum wind speed (horizontal arrows) and maximum upward motion (vertical arrows) along schematic wave-shaped trajectories for each flight, and the mean of all flights, for various periods of oscillation. In the mean for all flights it is seen that for most oscillation periods the speed was at a maximum ahead of the trough in the trajectory, the only exception being oscillations of a 45-min. period. Thus, if it is assumed that the large-scale air flow is nearly geostrophic and that small-scale geostrophic oscillations do not exist, then the tetroon moved faster when it was moving down the pressure gradient than when it was mov-

TABLE 4.—*Autocorrelation coefficients of tetroon speed (V), vertical motion (W), cross-stream (V_n) and along-stream (V_s), velocity components for Cape Hatteras flights*

Minutes	$R(V)$	$R(W)$	$R(V_n)$	$R(V_s)$	$\frac{1-R(V_s)}{1-R(V_n)}$
1	0.90	0.61	0.69	0.87	0.42
2	.81	.32	.40	.76	.40
3	.72	.12	.15	.67	.39
4	.62	−.10	−.10	.57	.39
5	.55	−.20	−.22	.49	.42
6	.52	−.23	−.27	.45	.43
7	.51	−.14	−.23	.45	.45
8	.50	−.10	−.18	.45	.47
9	.48	−.08	−.13	.46	.48
10	.47	−.07	−.06	.47	.50
12	.44	−.02	.01	.48	.53
14	.42	.02	.05	.45	.58
16	.38	.04	.09	.39	.67
18	.33	−.03	.09	.31	.76
20	.32	−.11	.04	.27	.76
24	.36	−.01	−.10	.31	.63
28	.23	.04	.01	.19	.82

ing up the pressure gradient. Thus, there is some evidence that kinetic energy (and momentum) is transported down the pressure gradient by these small-scale oscillations. Moreover, in the mean for all flights, the maximum upward motion of the tetroon took place near the trough line for oscillations of a period exceeding 18 min. and near the trajectory crest for oscillations of a smaller period. Thus, looking downstream the long-period tetroon oscillations were counterclockwise in a plane normal to the trajectory, while the shorter-period oscillations were clockwise. Insofar as the isotherms are parallel to the contours at this elevation, with cold air to the left of the flow looking downstream, this means that the long-period tetroon oscillations are direct (warm air rising, cold air sinking) while the short-period oscillations are indirect (cold air rising, warm air sinking). However, since, according to figure 11, the short-period tetroon oscillations in the vertical may not be representative of air oscillations in the vertical, the evidence for indirect circulations should be treated with caution. Further, until data on the temperature field are available on a comparable scale with the air motions here discussed, comparisons derived from synoptic-scale experience must be quite tentative.

F. SOME COMPARISONS WITH OTHER LAGRANGIAN DATA

Mean autocorrelation coefficients of the speed, V, vertical velocity, W, and cross-stream, V_n, and along-stream, V_s, components of tetroon velocity for the four Cape Hatteras flights are presented in table 4 for time lags from 1 to 28 min. Also presented in this table is the ratio of one minus the along-stream and one minus the cross-stream autocorrelation coefficients. It can be shown [10] that for Eulerian space correlation functions in the inertial range this ratio would be expected to be 0.6 for two-dimensional isotropic turbulence. It is of interest that in table 4 this ratio, while fluctuating between 0.4 and 0.8, does have a mean near 0.6, suggesting a certain similarity between Eulerian space and Lagrangian autocorrelation coefficients.

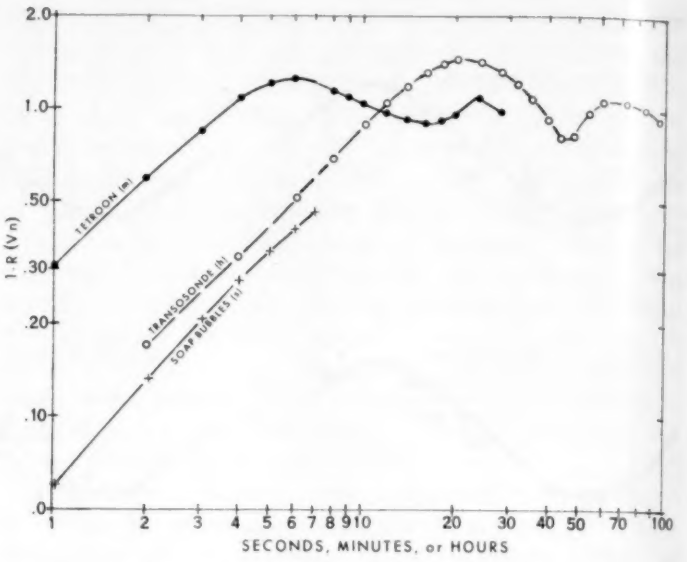

FIGURE 13.—Comparison of autocorrelation coefficients of the cross-stream velocity component obtained from Cape Hatteras tetroon flights, 300-mb. transosonde flights, and the soap bubble data of Edinger. (Note that the data are plotted on log-log paper, that the ordinate is in terms of one minus the autocorrelation coefficient, and that the abscissa is minutes, hours, and seconds, respectively, for the tetroon, transosonde, and soap bubble data.)

In figure 13 the value of one minus the cross-stream autocorrelation coefficient for the tetroon flights is plotted as a function of time on log-log paper. For purposes of comparison with other Lagrangian time scales, figure 13 also shows similar curves for the cross-stream velocity components as obtained from transosonde data [3] and the soap bubble data of Edinger [4]. Note that the abcissa in this figure represents seconds for the soap bubble data, minutes for the tetroon data, and hours for the transosonde data. It is seen that initially all three curves are approximately straight lines with slopes near 45° on the log-log plot, showing that for all three scales of motion $1-R(V_n) \propto t$ as would be anticipated from Lagrangian turbulence theory [11]. However, since pronounced periodicities are present in the cross-stream wind component along both the tetroon (17-min. period) and transosonde (46-hr. period) trajectories, the above proportionality between time and $1-R(V_n)$ soon breaks down. The soap bubbles could not be tracked for a length of time sufficient to delineate the predominant periodicity in that small-scale flow. Replacing the sign of proportionality by a sign of equality, we find that initially the autocorrelation coefficient for the tetroon data is given by

$$R(V_n)=1-4.9t/p_0 \tag{9}$$

while for the transosonde data it is given by

$$R(V_n)=1-3.7t/p_0 \tag{10}$$

where p_0 represents the predominant periodicities of oscillation (17 min., 46 hr.) cited above. These values for the constants differ from the theoretical Eulerian-time constants deduced by Ogura (1.67) and Gifford (1.18), and reported by Gifford [6], as would be expected. An interesting point is the ratio of these constants, 4.15 for the tetroons and 3.14 for the transosonde flights. Hay and Pasquill [8] have related Eulerian and Lagrangian turbulence statistics (on the assumption that the correlations decay with time in the same manner) by the factor β. They tabulated β values for a large range of scales together with the associated turbulence intensity. The scale of our experiments is intermediate between the diffusion experiments and the air trajectories they examined, and computed turbulence intensities for the tetroons (table 5) are also of the right order to fit this intermediate scale. Thus, these data do not contradict the use of a scale factor to relate Lagrangian and Eulerian data and indeed support the selection of a β value near 4.

It is also interesting to reverse the usual procedure and to work from these Lagrangian statistics to an estimate of Eulerian statistics. Following Gifford's [7] equation (6), one can estimate the position of the Eulerian spectral maximum. Such estimates from the tetroon flights indicate Eulerian maxima in the cross-wind component, V_n, between 12 and 43 cycles per hour, a frequency not in disagreement with the high frequency peak computed by Van der Hoven [15] for the Brookhaven tower data. The comparison suffers from a great difference in the height of the observations but it is, at least, not contradictory. The peak in the vertical spectra can be shifted in the same manner, giving Eulerian peaks at frequencies from 37 to 68 cycles per hour. Comparison of these values with those obtained by Jones [12] from wind inclination data at 2,000 ft. again shows reasonable agreement. (However, Jones' data do not extend far enough into the low frequency range to completely position his spectral peak.)

Taking into account the difficulties in positioning the tetroons previously discussed, one can examine the total variances in relation to any assumption of isotropy. From table 5 it is seen that in no case were the variances in the three components equally distributed and the lateral, V_n, to vertical, W, ratio ranged from about 2 to 4. Flight 3 is particularly interesting in this regard. It was the only nocturnal flight and indicates both reduced turbulence and a smaller V_n/W ratio.

6. CONCLUSION

The foregoing shows that data of interest and importance can be obtained from low-level tetroon flights even when the radar tracking is not too precise. During January 1960, eight tetroon flights were tracked by the excellent FPS–16 radar at the Wallops Island station of the National Aeronautics and Space Administration. The FPS–16 radar positions the tetroons with a root mean square error of only 5 yd., and for these flights radar range, azimuth, and elevation data were available at 10- or 30-sec. intervals. Consequently, information can be obtained from these flights on high frequency Lagrangian oscillations that could not possibly be obtained from the SP–1M radar. Thus, with the inclusion of transosonde data, information becomes available (admittedly at different elevations) concerning Lagrangian fluctuations with periods from a few tens of seconds to a week, with only a slight gap at periods of 3–8 hr. It is hoped that by passing tetroons from one radar station to another, reliable information can also be obtained on the Lagrangian fluctuations in this range. Such flights are next on the agenda. In addition, work is progressing on the development of a very light-weight transponder which can be attached to the tetroons in order to increase the tracking range. The future of the tetroon in air pollution studies, and other studies where knowledge of the Lagrangian wind fluctuations is essential, appears bright.

TABLE 5.—*Variance distribution and turbulence intensities*

Flight No.	Total variance (kt.²)			Average wind speed (kt.)	Turbulence intensity			
	$\sigma_{V_n}^2$	$\sigma_{V_e}^2$	σ_W^2	$\overline{V}$	$\sigma_{V_n}/\overline{V}$	$\overline{V}/\sigma_{V_n}$	$\sigma_W/\overline{V}$	$\overline{V}/\sigma_W$
2	40.8	4.0	10.6	23.0	0.28	3.6	0.14	7.1
3	6.9	7.8	3.1	26.3	.10	10.1	.07	14.9
5	18.7	5.6	4.9	10.2	.42	2.4	.22	4.6
Average	25.2	5.4	6.9	*17.7	.28	3.5	.16	6.8

*Weighted Average.

ACKNOWLEDGMENTS

Many organizations and individuals assisted in obtaining the experiments on which this work was based. Among these were the Weather Bureau Offices at Oak Ridge, Las Vegas, Idaho Falls, and Hatteras; the Lockheed Aircraft Corporation; and the U.S. Air Force, Air Defense Command. Special thanks are due Mr. Henry J. Mastenbrook, Naval Research Laboratory, for arranging and assisting the maiden flight at the Chesapeake Bay Annex, and Mr. R. R. Soller whose ingenuity and efforts enabled the development of routine launching techniques. Mrs. M. Hodges performed many of the tedious calculations.

REFERENCES

1. A. D. Anderson, H. J. Mastenbrook, and H. D. Cubbage, "The Transosonde—A New Meteorological Data-Gathering System," *NRL Report* No. 4649, U.S. Navy, Naval Research Laboratory, Washington, D.C., 1955, 18 pp.
2. J. K. Angell, "A Climatological Analysis of Two Years of Routine Transosonde Flights from Japan," *Monthly Weather Review*, vol. 87, No. 12, Dec. 1959, pp. 427–439.
3. J. K. Angell, A Study of Lagrangian Wind Fluctuations Derived from Transosonde Data, Unpublished Manuscript, U.S. Weather Bureau, 1957, 41 pp.
4. J. G. Edinger, "A Technique for Measuring the Detailed Structure of Atmospheric Flow," *Geophysical Research Papers* No. 19, U.S. Air Force Cambridge Research Center, Geophysics Research Directorate, 1952, pp. 241–261.

562159—60——3

5. G. Emmons, B. Haurwitz, and A. F. Spilhaus, "Oscillations in the Stratosphere and High Troposphere," *Bulletin of the American Meteorological Society*, vol. 31, No. 4, Apr. 1950, pp. 135–138.
6. F. A. Gifford, "The Relation Between Space and Time Correlations in the Atmosphere," *Journal of Meteorology*, vol. 13, No. 3, June 1956, pp. 289–294.
7. F. A. Gifford, "A Simultaneous Lagrangian-Eulerian Turbulence Experiment," *Monthly Weather Review*, vol. 83, No. 12, Dec. 1955, pp. 293–301.
8. J. S. Hay and F. Pasquill, "Diffusion from a Continuous Source in Relation to the Spectrum and Scale of Turbulence," *Advances in Geophysics*, vol. 6, Academic Press, New York, N.Y., 1959, pp. 345–365.
9. J. Holmboe, G. E. Forsythe, and W. Gustin, *Dynamic Meteorology*, John Wiley and Sons, Inc., New York, 1945, 378 pp.
10. J. W. Hutchings, "Turbulence Theory Applied to Large Scale Atmospheric Phenomena," *Journal of Meteorology*, vol. 12, No. 3, June 1955, pp. 263–271.
11. E. Inoue, "On the Lagrangian Correlation Coefficient for Turbulent Diffusion and Its Application to Atmospheric Diffusion Phenomena," *Geophysical Research Papers* No. 19, U.S. Air Force Cambridge Research Center, Geophysics Research Directorate, 1952, pp. 397–411.
12. J. I. P. Jones, "Studies of Eddy Structure in the First Few Thousand Feet of the Atmosphere, Part 2, A Preliminary Examination of the Spectrum and Scale of the Vertical Component at 2000 feet," *Porton Technical Paper* No. 588, Chemical Defence Experimental Establishment, Porton, Wilts, February 1957. (Also issued by Great Britain, Meteorological Research Committee as *M.R.P.* 1044.)
13. H. T. Mantis, "Meteorological Studies Using Constant Altitude Balloons," *Technical Report* No. AP–14, School of Physics, University of Minnesota, Minneapolis, Minn., 1959.
14. J. W. Tukey, "The Sampling Theory of Power Spectrum Estimates," *Symposium on Application of Autocorrelation Analysis to Physical Problems*, U.S. Navy, Office of Naval Research, 1950, pp. 47–67.
15. I. Van der Hoven, "Power Spectrum of Horizontal Wind Speed in the Frequency Range from 0.0007 to 900 Cycles Per Hour," *Journal of Meteorology*, vol. 14, No. 2, Apr. 1957, pp. 160–164.
16. I. Van der Hoven and H. A. Panofsky, "Statistical Properties of the Vertical Flux and Kinetic Energy at 100 Meters," Final Report on Contract AF 19(604)–166, Dept. of Meteorology, The Pennsylvania State University, June 1954, 55 pp.

APPENDIX

A. Weigh-off procedure assuming tetroon of constant volume
   1. Determine surface tetroon volume (V_s) from equation (4).
   2. Determine density surface (ρ_a) at which flight is to be made.
   3. Determine helium density (ρ_{hs}) at earth's surface from equation of state for helium.
   4. Weight to be added to tetroon equals $V_s(\rho_a-\rho_{hs})-W_b$ where W_b is weight of tetroon.

B. Weigh-off procedure for low-level tetroon flights assuming tetroon volume varies according to equation (5)
   1. Determine surface tetroon volume (V_s) from equation (4).
   2. Determine density surface (ρ_a) at which flight is to be made.
   3. Determine tetroon superpressure (Δp) at density surface of flight assuming tetroon released in fully inflated state.
   4. Determine tetroon volume at flight level (V_e) from $V_e=V_s+.0038(e^{0.015\Delta p}-1)$
   5. Weight to be added to tetroon equals $V_e\rho_a-V_s\rho_{hs}-W_b$ where ρ_{hs} is surface helium density and W_b is tetroon weight.

C. Weigh-off procedure for high-level tetroon flights (tetroon partially deflated at the earth's surface) assuming tetroon volume varies according to equation (5)
   1. Determine surface tetroon volume (V_s) from equation (4).
   2. Determine density surface (ρ_a) at which flight is to be made.
   3. Determine what volume of helium (V_h) would fully inflate tetroon at flight level plus Δp, where Δp is less than 100 mb.:

$$V_h=\frac{V_s\rho_{a+\Delta p}}{\rho_{as}}$$

   where ρ_{as} is surface air density and $\rho_{a+\Delta p}$ is air density when tetroon fully inflated.
   4. Deflate tetroon until free lift of tetroon equals

$$V_h(\rho_{as}-\rho_{hs})-W_b$$

   where ρ_{hs} is surface helium density and W_b is tetroon weight.
   5. Determine tetroon volume at flight level (V_e) from

$$V_e=V_s+0.0038(e^{0.015\Delta p}-1)$$

   6. Weight to be added to tetroon equals $V_e\rho_a-V_h\rho_{hs}-W_b$

Notes:
1. The selection of a desired flight altitude cannot be entirely arbitrary for the "deflated" tetroon (Method C) since enough free lift (contained helium) must be retained to escape surface turbulence and clear obstacles in the launching area.
2. There is evidence that marked temperature inversions can inhibit, or even prevent, a "deflated" tetroon from achieving the chosen flight level by radically altering the air vs. helium density relationships compared to surface inflation conditions. This phenomenon is under study.

AN EXTENSION OF A TABLE OF ABSORPTION FOR ELSASSER BANDS*

D. Q. WARK AND M. WOLK

U.S. Weather Bureau, Washington, D.C.

[Manuscript received July 19, 1960; revised July 25, 1960]

Elsasser [1] formulated the absorption by a band consisting of Lorentz-shaped lines equally spaced and of equal strengths. He found the mean absorption over a spectral interval D, the spacing between the lines, and through a homogeneous gas of path length u, to be

$$A=\sinh\beta\int_0^y \exp(-y\cosh\beta)\,J_0(iy)dy \qquad (1)$$

where $\beta=2\pi\alpha/D$

and $y=(Su)/(D\sinh\beta)$

in which α is the half width of the lines at half maximum and S is the strength (integrated absorption coefficient) of an individual line.

Kaplan [2] has shown that equation (1) may be represented by

$$A=\sinh\beta\exp(-y)\left[J_0(iy)\sum_{n=1}^{\infty}a_n y^n+i\,J_1(iy)\sum_{n=1}^{\infty}b_n y^n\right] \qquad (2)$$

in which $a_1=1$

$$b_1=-\beta/\sinh\beta,\quad \cosh\beta<3$$

$$nb_{n+1}=b_n+a_n$$

$$na_n=a_{n-1}+b_{n-1}+(-1)^{n+1}c^{n-1}/(n-1)!$$

where $c=\cosh\beta-1$

From this expansion Kaplan prepared a table of fractional absorption, in which β ranges from 0.01 to 1.0 and y from 0 to 40.

Radiative transfer problems arising in meteorology require an extension of the table. In the present work, therefore, the series solution of Kaplan has been employed to carry the table to the limits normally encountered in the atmosphere. Calculations were performed for $\beta=1.0$, 0.1, 0.01, and 0.001. As many as 60 decimal places were required in the evaluation of the coefficients. Exponential functions of the desired accuracy were obtained from Van Orstrand's [3] tables.

The ranges of y were 0 to 150,000 or to the point where A became unity to four decimal places. For intermediate values of β, an interpolation scheme was devised to determine the difference between the correct values of A and the error function approximation,

$$A=\mathrm{erf}\,(\beta\sqrt{y/2}\,) \qquad (3)$$

Table 1 shows the results of this work. The calculated values of A are exact to the accuracy shown. The interpolated values should be correct to within 0.0001 in most cases. All values of A lying outside this table, except for $\beta>1.0$, can be calculated precisely to at least four decimal places from the error function approximation. Kaplan's table has been included as a part of table 1.

*This work was supported by the National Aeronautics and Space Administration.

REFERENCES

1. W. M. Elsasser, "Mean Absorption and Equivalent Absorption Coefficients," *Physical Review*, vol. 54, No. 2, July 15, 1938, pp. 126–129.
2. L. D. Kaplan, "Regions of Validity of Various Absorption-Coefficient Approximations," *Journal of Meteorology*, vol. 10, No. 2, April 1953, pp. 100–104.
3. C. E. van Orstrand, "Tables of the Exponential Function and of the Circular Sine and Cosine to Radian Argument," *Memoirs of the National Academy of Sciences*, vol. XIV, Fifth Memoir, 1925, 79 pp.

TABLE 1.—*Fractional absorption by an Elsasser band, with arguments y and β*

y \ β	.0001	.0002	.0003	.0004	.0006	.0008	.001	.002	.003	.004	.006	.008	.01	.02	.03	.04	.06	.08	.10	.2	.3	.4	.5	.6	.7	.8	.9	1.0	β/y
.02	.0000	.0000	.0000	.0000	.0000	.0000	.0000	.0000	.0001	.0001	.0001	.0002	.0002	.0004	.0006	.0008	.0012	.0016	.0020	.0040	.0060	.0081	.0103	.0126	.0150	.0175	.0202	.0231	.02
.04	.0000	.0000	.0000	.0000	.0000	.0000	.0000	.0001	.0001	.0002	.0002	.0003	.0004	.0008	.0012	.0016	.0024	.0031	.0039	.0079	.0119	.0161	.0204	.0249	.0296	.0346	.0399	.0456	.04
.06	.0000	.0000	.0000	.0000	.0000	.0000	.0001	.0001	.0002	.0002	.0004	.0005	.0006	.0012	.0017	.0023	.0035	.0047	.0058	.0117	.0177	.0239	.0302	.0369	.0439	.0512	.0590	.0674	.06
.08	.0000	.0000	.0000	.0000	.0000	.0001	.0001	.0002	.0002	.0003	.0005	.0006	.0008	.0015	.0023	.0031	.0046	.0062	.0077	.0155	.0234	.0315	.0399	.0486	.0578	.0674	.0774	.0885	.08
.10	.0000	.0000	.0000	.0000	.0001	.0001	.0001	.0002	.0003	.0004	.0006	.0008	.0010	.0019	.0029	.0038	.0057	.0076	.0095	.0192	.0289	.0390	.0493	.0601	.0714	.0832	.0957	.1090	.10
.15	.0000	.0000	.0000	.0001	.0001	.0001	.0002	.0002	.0003	.0004	.0008	.0011	.0014	.0028	.0042	.0056	.0084	.0112	.0140	.0281	.0424	.0570	.0720	.0876	.1039	.1209	.1388	.1577	.15
.2	.0000	.0000	.0000	.0001	.0001	.0002	.0002	.0004	.0005	.0007	.0010	.0014	.0018	.0036	.0055	.0073	.0109	.0146	.0182	.0365	.0551	.0741	.0936	.1137	.1346	.1563	.1791	.2029	.2
.3	.0000	.0000	.0001	.0001	.0002	.0002	.0003	.0006	.0008	.0011	.0015	.0022	.0026	.0052	.0078	.0104	.0157	.0209	.0261	.0524	.0790	.1060	.1335	.1618	.1909	.2210	.2520	.2841	.3
.4	.0000	.0001	.0001	.0001	.0002	.0003	.0003	.0007	.0010	.0013	.0020	.0027	.0033	.0067	.0100	.0133	.0200	.0267	.0334	.0669	.1007	.1350	.1698	.2052	.2414	.2783	.3161	.3548	.4
.5	.0000	.0001	.0001	.0002	.0002	.0003	.0004	.0008	.0012	.0015	.0024	.0032	.0040	.0080	.0120	.0160	.0240	.0321	.0401	.0803	.1208	.1615	.2028	.2445	.2867	.3295	.3728	.4165	.5
.6	.0001	.0001	.0001	.0002	.0003	.0004	.0005	.0009	.0014	.0018	.0027	.0037	.0046	.0093	.0139	.0185	.0278	.0370	.0463	.0927	.1392	.1860	.2330	.2802	.3277	.3754	.4231	.4707	.6
.7	.0001	.0001	.0002	.0002	.0003	.0004	.0005	.0010	.0015	.0020	.0030	.0041	.0052	.0104	.0156	.0208	.0312	.0417	.0521	.1042	.1563	.2085	.2607	.3129	.3649	.4167	.4680	.5185	.7
.8	.0001	.0001	.0002	.0002	.0003	.0005	.0006	.0011	.0016	.0022	.0034	.0045	.0057	.0115	.0172	.0230	.0345	.0460	.0575	.1149	.1723	.2295	.2864	.3429	.3988	.4540	.5081	.5609	.8
.9	.0001	.0002	.0002	.0002	.0004	.0005	.0006	.0013	.0019	.0024	.0036	.0049	.0063	.0125	.0188	.0250	.0375	.0501	.0626	.1250	.1872	.2489	.3101	.3705	.4299	.4879	.5443	.5986	.9
1.0	.0001	.0002	.0002	.0003	.0004	.0005	.0007	.0014	.0020	.0026	.0040	.0053	.0067	.0135	.0202	.0269	.0404	.0539	.0673	.1345	.2011	.2672	.3323	.3961	.4584	.5188	.5769	.6322	1.0
1.5	.0001	.0002	.0003	.0004	.0005	.0007	.0009	.0018	.0026	.0035	.0053	.0070	.0088	.0176	.0264	.0352	.0528	.0703	.0878	.1749	.2605	.3437	.4239	.5004	.5724	.6394	.7007	.7592	1.5
2	.0001	.0002	.0003	.0005	.0006	.0008	.0011	.0020	.0031	.0042	.0063	.0083	.0105	.0209	.0314	.0419	.0628	.0837	.1045	.2076	.3077	.4036	.4940	.5778	.6541	.7222	.7819	.8328	2
3	.0001	.0003	.0004	.0006	.0008	.0011	.0013	.0027	.0040	.0052	.0079	.0106	.0132	.0264	.0396	.0527	.0791	.1053	.1314	.2596	.3817	.4949	.5973	.6872	.7639	.8273	.8780	.9170	3
4	.0002	.0003	.0005	.0006	.0010	.0012	.0015	.0031	.0046	.0062	.0093	.0124	.0154	.0309	.0463	.0617	.0924	.1230	.1534	.3016	.4398	.5642	.6720	.7619	.8338	.8888	.9291	.9570	4
5	.0002	.0004	.0005	.0007	.0011	.0014	.0017	.0035	.0053	.0069	.0105	.0140	.0174	.0347	.0521	.0694	.1040	.1383	.1725	.3374	.4882	.6197	.7292	.8158	.8808	.9270	.9579	.9772	5
6	.0002	.0004	.0006	.0008	.0012	.0016	.0019	.0038	.0058	.0076	.0115	.0153	.0191	.0382	.0573	.0764	.1144	.1521	.1895	.3689	.5296	.6657	.7744	.8560	.9135	.9514	.9746	.9877	6
7	.0002	.0004	.0006	.0008	.0013	.0017	.0021	.0041	.0062	.0082	.0125	.0166	.0207	.0414	.0621	.0827	.1238	.1646	.2050	.3972	.5659	.7045	.8108	.8866	.9367	.9674	.9845	.9933	7
8	.0002	.0005	.0007	.0009	.0014	.0018	.0022	.0044	.0067	.0089	.0134	.0179	.0222	.0444	.0665	.0886	.1326	.1762	.2193	.4229	.5981	.7377	.8405	.9102	.9534	.9779	.9908	.9963	8
9	.0002	.0005	.0007	.0010	.0014	.0019	.0024	.0048	.0071	.0095	.0142	.0190	.0236	.0472	.0707	.0942	.1409	.1871	.2327	.4465	.6269	.7664	.8650	.9285	.9655	.9853	.9943	.9981	9
10	.0003	.0005	.0008	.0010	.0015	.0020	.0025	.0050	.0075	.0100	.0149	.0200	.0249	.0498	.0746	.0994	.1486	.1973	.2452	.4683	.6529	.7914	.8854	.9429	.9744	.9899	.9964	.9989	10
11	.0003	.0005	.0008	.0011	.0016	.0021	.0026	.0053	.0079	.0105	.0157	.0210	.0262	.0523	.0783	.1043	.1560	.2069	.2571	.4887	.6765	.8133	.9024	.9542	.9807	.9928	.9975	.9992	11
12	.0003	.0006	.0008	.0011	.0017	.0022	.0027	.0055	.0083	.0110	.0165	.0220	.0273	.0547	.0819	.1091	.1630	.2161	.2683	.5077	.6980	.8325	.9168	.9631	.9852	.9947	.9982	.9994	12
13	.0003	.0006	.0009	.0012	.0017	.0023	.0028	.0058	.0086	.0114	.0171	.0228	.0285	.0569	.0853	.1136	.1697	.2249	.2790	.5256	.7177	.8496	.9288	.9700	.9886	.9961	.9988	.9996	13
14	.0003	.0006	.0009	.0012	.0018	.0024	.0030	.0060	.0090	.0119	.0178	.0237	.0296	.0591	.0886	.1179	.1761	.2333	.2893	.5424	.7358	.8646	.9391	.9757	.9913	.9971	.9991	.9998	14
15	.0003	.0006	.0009	.0012	.0019	.0025	.0031	.0062	.0093	.0123	.0184	.0245	.0306	.0612	.0917	.1221	.1823	.2414	.2892	.5583	.7525	.8780	.9478	.9802	.9932	.9978	.9993	.9999	15
16	.0003	.0006	.0010	.0013	.0019	.0026	.0032	.0064	.0096	.0128	.0191	.0253	.0317	.0633	.0948	.1261	.1882	.2492	.3086	.5734	.7679	.8900	.9552	.9842	.9954	.9985	.9997	1.0000	16
20	.0004	.0007	.0011	.0014	.0021	.0028	.0035	.0071	.0107	.0143	.0213	.0284	.0354	.0708	.1061	.1411	.2104	.2779	.3434	.6267	.8192	.9265	.9752	.9930	.9983	.9996	1.0000		20
30	.0004	.0009	.0013	.0018	.0026	.0035	.0044	.0087	.0131	.0175	.0261	.0349	.0435	.0869	.1300	.1727	.2566	.3374	.4147	.7255	.8995	.9719	.9940	.9990	.9997	1.0000			30
40	.0005	.0010	.0015	.0020	.0030	.0040	.0050	.0101	.0151	.0202	.0302	.0403	.0503	.1003	.1500	.1991	.2948	.3861	.4718	.7934	.9423	.9890	.9986	.9998	1.0000				40
50	.0006	.0011	.0017	.0022	.0034	.0045	.0056	.0113	.0169	.0226	.0337	.0450	.0562	.1122	.1676	.2221	.3278	.4275	.5196	.8424	.9665	.9955	.9996	1.0000					50
60	.0006	.0012	.0019	.0025	.0037	.0050	.0062	.0124	.0185	.0247	.0370	.0493	.0616	.1228	.1834	.2428	.3572	.4638	.5606	.8785	.9801	.9981	.9999						60
70	.0007	.0013	.0020	.0027	.0040	.0053	.0067	.0133	.0200	.0267	.0399	.0533	.0666	.1327	.1979	.2617	.3837	.4960	.5966	.9056	.9881	.9991	1.0000						70
80	.0007	.0014	.0021	.0028	.0043	.0057	.0071	.0143	.0214	.0285	.0427	.0569	.0712	.1418	.2113	.2790	.4080	.5252	.6284	.9263	.9928	.9996							80
90	.0008	.0015	.0023	.0030	.0045	.0060	.0076	.0151	.0227	.0303	.0454	.0604	.0755	.1503	.2238	.2953	.4303	.5517	.6568	.9423	.9957	.9999							90
100	.0008	.0016	.0024	.0032	.0048	.0064	.0080	.0160	.0239	.0319	.0478	.0637	.0796	.1583	.2355	.3105	.4511	.5759	.6822	.9547	.9974	1.0000							100
150	.0010	.0020	.0029	.0039	.0059	.0078	.0098	.0195	.0293	.0391	.0586	.0779	.0974	.1932	.2864	.3755	.5372	.6724	.7791	.9857	.9998								150
200	.0011	.0022	.0034	.0045	.0068	.0090	.0113	.0226	.0338	.0451	.0676	.0900	.1124	.2226	.3284	.4282	.6037	.7420	.8426	.9955	1.0000								200
300	.0014	.0028	.0042	.0055	.0083	.0111	.0138	.0276	.0414	.0552	.0828	.1101	.1374	.2709	.3966	.5115	.7013	.8342	.9168	.9995									300
400	.0016	.0032	.0048	.0064	.0096	.0128	.0160	.0319	.0478	.0638	.0955	.1271	.1585	.3109	.4514	.5763	.7699	.8904	.9544	.9999									400
500	.0018	.0036	.0054	.0071	.0107	.0143	.0178	.0357	.0535	.0713	.1037	.1420	.1769	.3453	.4977	.6289	.8203	.9263	.9747	1.0000									500
600	.0020	.0039	.0059	.0078	.0117	.0156	.0195	.0391	.0586	.0780	.1168	.1554	.1937	.3758	.5376	.6729	.8584	.9501	.9857										600
700	.0021	.0042	.0063	.0084	.0127	.0169	.0211	.0422	.0633	.0843	.1261	.1676	.2088	.4033	.5727	.7101	.8876	.9658	.9919										700
800	.0022	.0045	.0068	.0090	.0135	.0180	.0226	.0451	.0676	.0901	.1348	.1790	.2227	.4284	.6039	.7422	.9103	.9764	.9950										800
900	.0024	.0048	.0072	.0096	.0144	.0192	.0239	.0478	.0717	.0955	.1428	.1897	.2358	.4515	.6319	.7699	.9282	.9837	.9973										900
1000	.0025	.0050	.0076	.0101	.0151	.0202	.0252	.0504	.0756	.1007	.1505	.1997	.2481	.4729	.6572	.7942	.9423	.9886	.9984										1000
1500	.0031	.0062	.0093	.0124	.0185	.0247	.0309	.0617	.0925	.1231	.1838	.2433	.3014	.5614	.7548	.8787	.9799	.9981	.9999										1500
2000	.0036	.0071	.0107	.0143	.0214	.0285	.0357	.0713	.1067	.1420	.2116	.2795	.3453	.6289	.8203	.9264	.9927	.9997	1.0000										2000
3000	.0044	.0087	.0131	.0175	.0262	.0350	.0437	.0872	.1305	.1734	.2576	.3387	.4161	.7267	.8996	.9716	.9990												3000
4000	.0050	.0101	.0151	.0202	.0303	.0404	.0504	.1006	.1505	.1997	.2957	.3871	.4729	.7941	.9422	.9886	.9998												4000
5000	.0056	.0113	.0169	.0226	.0338	.0451	.0564	.1125	.1680	.2227	.3286	.4284	.5205	.8427	.9661	.9953	1.0000												5000
6000	.0062	.0124	.0185	.0247	.0371	.0494	.0617	.1231	.1837	.2433	.3579	.4645	.5614	.8787	.9799	.9981													6000
7000	.0067	.0133	.0200	.0267	.0400	.0534	.0667	.1329	.1982	.2621	.3843	.4967	.5972	.9058	.9879	.9992													7000
8000	.0071	.0143	.0214	.0285	.0428	.0570	.0713	.1420	.2116	.2795	.4085	.5257	.6289	.9264	.9927	.9996													8000
9000	.0076	.0151	.0227	.0303	.0454	.0605	.0756	.1505	.2240	.2957	.4308	.5521	.6572	.9422	.9956	.9998													9000
10000	.0080	.0160	.0239	.0319	.0478	.0638	.0797	.1585	.2358	.3108	.4515	.5763	.6827	.9545	.9973	.9999													10000
2×10^4	.0113	.0226	.0338	.0451	.0676	.0901	.1125	.2227	.3286	.4284	.6038	.7421	.8427	.9953	1.0000	1.0000													2×10^4
3×10^4	.0138	.0276	.0414	.0552	.0828	.1102	.1375	.2710	.3967	.5116	.7013	.8341	.9167	.9995															3×10^4
4×10^4	.0160	.0319	.0478	.0638	.0955	.1271	.1585	.3108	.4515	.5763	.7699	.9104	.9545	.9999															4×10^4
5×10^4	.0178	.0357	.0535	.0713	.1067	.1420	.1769	.3453	.4977	.6289	.8203	.9264	.9747	1.0000															5×10^4
6×10^4	.0196	.0391	.0586	.0780	.1168	.1554	.1935	.3758	.5376	.6728	.8584	.9500	.9857																6×10^4
7×10^4	.0211	.0422	.0633	.0843	.1261	.1676	.2087	.4033	.5726	.7101	.8876	.9657	.9918																7×10^4
8×10^4	.0226	.0451	.0676	.0901	.1348	.1790	.2227	.4284	.6039	.7421	.9103	.9764	.9953																8×10^4
9×10^4	.0239	.0478	.0717	.0955	.1428	.1897	.2358	.4515	.6319	.7699	.9281	.9835	.9973																9×10^4
10×10^4	.0252	.0504	.0756	.1006	.1505	.1997	.2482	.4729	.6572	.7941	.9422	.9885	.9984																10×10^4
15×10^4	.0309	.0617	.0925	.1231	.1838	.2433	.3015	.5614	.7547	.8787	.9799	.9980	.9999																15×10^4

EXTRAPOLATION TO THE 50-MB. LEVEL FROM 100-MB. DATA IN ANTARCTICA*

WILLIAM S. WEYANT

U.S. Weather Bureau, Washington, D.C.

[Manuscript received June 17, 1960; revised July 21, 1960

ABSTRACT

Winter-month data obtained at United States Antarctic stations during the IGY are used to compute coefficients for regression equations relating the 100-mb. temperatures and heights to the 50-mb. heights. It is found upon trial that the layer thickness can be estimated as accurately from the 100-mb. temperature alone as from both the temperature and 100-mb. height; therefore, the simpler equations in only one variable are used. The average errors in computed heights are less than 2 dekameters and the extreme errors 6 dkm. or less when tests are performed on independent data.

A measure of the average lapse rates within the layer between 100 mb. and 50 mb., derived from the same data as the equations mentioned above, proves to be as good a predictor as any of the regression equations. These mean lapse rates show a regular variation with both latitude and month. The largest values (greatest instability) occur in the coldest months and the highest latitudes, and the greatest layer stability in lower latitudes and warmer months.

Additional 50-mb. heights are extrapolated from the observed 100-mb. data for all of the stations considered for radiosonde ascents reaching 100 mb. but not 50 mb.; means of the computed heights are compared with the means of the observed 50-mb. heights to determine if any bias in the observations can be demonstrated.

1. INTRODUCTION

During the International Geophysical Year in the Antarctic, regular radiosonde ascents at 12-hour intervals were made at, inter alia, the United States stations at the South Pole, Byrd, Little America, McMurdo Sound, Ellsworth, and Wilkes, and at the joint New Zealand-United States station at Hallett. In the colder six months of the year, April to September, and in particular during the four winter months from May to August, a large percentage of those ascents were terminated between 100 mb. and 50 mb., usually due to balloon bursts. The 50-mb. height data can be considerably augmented by an extrapolative technique to obtain reasonably accurate values of 50-mb. heights from the 100-mb. data.

The purpose of this investigation is to find the most feasible method of obtaining additional 50-mb. data by extrapolation from observed 100-mb. data, and to examine the thermal structure of the 100 mb. to 50 mb. layer and its variations with latitude and month over the Antarctic during the period considered.

2. EXTRAPOLATIVE METHODS

The first approach to the problem was to find coefficients for the regression equations relating the 50-mb. height, H_{50}, to the 100-mb. height, H_{100}, and the 100-mb. temperature, T_{100}. This is the same procedure followed by previous investigators in the Northern Hemisphere, as for example, Hering and Antanaitis [1], and currently in use by the U.S. Weather Bureau Stratospheric Analysis Project. Since in all cases we are to work from known 100-mb. data, the 50-mb. height is completely determined by the known 100-mb. height and the thickness, H_d, of the 100 mb. to 50 mb. layer. The original regression equations,

$$H_{50}=A_1H_{100}+A_2T_{100}+A_0 \tag{1}$$

may then be transformed to equations of the form

$$H_d=A_1'H_{100}+A_2T_{100}+A_0, \tag{2}$$

where $A_1'=A_1-1$.

The coefficients for equation (2) were computed for Little America for the six months April to September 1957 (228 ascents) to give a range through the period, and for the month of June 1957 for Little America, South Pole, Byrd and Wilkes (131 ascents) to give a range in latitude. The resulting A_1 coefficients showed a range of from -0.05 to $+0.015$, and none was significantly different from zero. Therefore, a new set of regression equations was obtained from this same data by computing the A_2' and A_0' coefficients for the general equation

$$H_d=A_2'T_{100}+A_0'. \tag{3}$$

A test of equations (2) and (3) on a limited amount of independent data (26 cases) resulted in an average error of 13 gpm. in the 50-mb. height using (2) and 11 gpm.

* Paper presented at the Antarctic Symposium of Buenos Aires, November 1959.

TABLE 1.—*Mean values of thickness of 100 mb. to 50 mb. layer (H_d) and 100-mb. temperature (T_{100}) for winter months in the Antarctic. Thicknesses are in geopotential meters and temperatures in degrees Celsius.*

		South Pole (90° S.)	Byrd (80° S.)	Little America V—Ellsworth (78° S.)	Hallett (72° S.)	Wilkes (66° S.)	Monthly mean
April	H_d	----------	4291	4324	4384	4432	4343
	T_{100}	----------	−58.6	−57.5	−55.0	−53.1	−56.6
May	H_d	4064	4081	4122	4266	4350	4164
	T_{100}	−69.1	−68.3	−66.4	−59.6	−57.3	−64.6
June	H_d	3943	3977	4032	4114	4275	4050
	T_{100}	−74.8	−73.1	−71.1	−67.6	−60.4	−70.2
July	H_d	3852	3888	3896	4009	4038	3931
	T_{100}	−79.1	−77.4	−77.3	−72.2	−71.3	−75.7
August	H_d	3780	3821	3874	3946	4041	3880
	T_{100}	−83.4	−81.9	−79.3	−75.6	−71.9	−79.0
Sept.	H_d	3863	3902	3961	4113	4156	3988
	T_{100}	−81.0	−79.5	−76.5	−70.3	−69.1	−75.7
Mean (Lat.)	H_d	3969	3992	4033	4138	4214	(4058.26)
	T_{100}	−74.2	−73.2	−71.4	−66.8	−63.9	(−70.33)

using (3). On the basis of this comparison, it was decided to use equations of the form (3) in computing regression coefficients for all stations except McMurdo Sound, and for all months of 1957 and 1958 (April to September) in which at least 8 ascents reached the 50-mb. level. The data from Ellsworth Station and Little America were combined, since these two stations are approximately the same latitude; a detailed listing of the data used is given by the parenthetical values in table 4 in the rows headed "Comp.". The McMurdo Sound data and unused data from the remaining stations were reserved for testing the results; table 3 gives a breakdown of the independent data by station and month.

In the course of the above computations, intermediate steps made it convenient to extract from the data the mean H_d and T_{100} for each station and month (table 1), and also to compute some of the correlation coefficients between these two parameters. The latter were generally quite high, ranging from +0.89 to +0.99 with a median value of those computed (18) of +0.95. Since the original computations were based on only 1455 cases in all, and individual station-months on from 8 to 43 ascents, it was thought advisable to test on independent data not only for the regression equations but also for equations based on the assumption of a constant lapse-rate of temperature within the layer.

If we assume that there is no significant amount of moisture within the layer from 100 mb. to 50 mb., then the mean virtual temperature and the mean temperature of the layer are approximately equal. The general equation which relates the thickness, H_d (in geopotential meters) and the mean virtual temperature, $\overline{T}_v$ (in ° K.) of a layer of air between two constant pressure surfaces p_1 (base) and p_2 (top) is

$$H_d = 67.442\ \overline{T}_v \log_{10}(p_1/p_2)$$

TABLE 2.—*Computed lapse rate, °C./km., of 100 mb. to 50 mb. layer.*

	South Pole (90° S.)	Byrd (80° S.)	Little America V—Ellsworth (78° S.)	Hallett (72° S.)	Wilkes (66° S.)	Monthly mean
April	−1.5	−1.5	−1.2	−1.0	−0.8	−1.21
May	−1.9	−1.9	−1.8	−1.6	−0.7	−1.65
June	−2.1	−2.1	−1.7	−1.4	−1.0	−1.72
July	−2.2	−2.0	−2.0	−1.7	−1.5	−1.96
August	−1.9	−1.6	−1.6	−1.6	−1.1	−1.59
September	−1.0	−0.7	−0.8	−0.1	+0.3	−.79
Mean for station (Latitude)	−1.74	−1.66	−1.53	−1.25	−.79	−1.44

as given, for example, in [2]. We may now write for the 100 mb. to 50 mb. layer, substituting the mean temperature, $\overline{T}_k$, for the mean virtual temperature, the equation

$$H_d = 20.302\ \overline{T}_k. \tag{4}$$

If we now make the further assumptions that the lapse rate is constant with height within the layer and with time over the period of a month at a given station, then these lapse rates can be computed from the data given in table 1. The computed mean lapse rate, ($\overline{\Gamma}_d$), for each station and month, as well as the weighted mean lapse rates for each month and latitude, are given in table 2.

For extrapolation of the 50-mb. heights, we may now write a set of equations, based on the assumption of constant lapse rates, of the form

$$H_d = 20.302\left[273.16 + T_{100} + \frac{\Gamma_d H_d}{2000}\right] \tag{5}$$

This is the same as equation (4) with the term inside the brackets representing the mean absolute temperature of the layer for a given T_{100} (in °C.) if the assumption of constant lapse rate holds.

3. TESTS ON INDEPENDENT DATA

Independent data from the four months, May to August, were used to test four different methods of extrapolating the 50-mb. heights from the 100-mb. data, as follows:

Method I used equations of form (3) for a given latitude and month applied to data from the same latitude and month; Method II used equations of the form (3) for a given latitude, with the coefficients computed by combining the data from the four months, May to August, applied to data from the same latitude; Method III used equations of the form (3) for a given month, with the coefficients computed by combining all data for that month, applied to all independent data for the given month; Method IV was based on equations of the form (5), although to facilitate computations a nomogram and two graphs based on these equations, as described in the next section, were actually used.

The results of the testing of these various extrapolative

TABLE 3.—*Results of tests of four extrapolative methods on independent data.*

Station	Months	No. of cases	Mean errors (gpm.) in computed 50-mb. height			
			Method I	Method II	Method III	Method IV
75°–90°S.						
Pole	May and Aug., 1958	15	8.8	15.7	18.0	10.7
Byrd	May to Aug., 1958	97	12.2	12.4	15.1	12.2
Ellsworth	May to Aug., 1957	28	11.8	10.7	13.6	14.0
McMurdo	May to Aug., 1957	165	14.8	12.7	14.7	12.8
Mean		(305)	13.4	12.5	14.9	12.6
North of 75°S.						
Hallett	May, June and Aug. 1958.	74	22.5	23.1	25.3	22.6
Wilkes	May-Aug. 1958	79	19.8	(Independent for Method I only: not included in mean below)		
Mean		(379)	15.2	14.6	16.9	14.5

methods of obtaining the 50-mb. height are shown in table 3. The best results were obtained by using Method IV, although the small difference between this mean error and that from Method II hardly can be significant. In the area from latitude 77° S. to the Pole, the average errors using Method I, II, or IV were quite consistently between 10 and 15 gpm., while from Hallett northward more limited amounts of independent data indicated an average error using the best methods of 20 to 25 gpm. In general, the extreme error was about four times the average error.

4. CONSTRUCTION OF NOMOGRAM AND GRAPHS

When we substitute in equation (5) the values for the layer thickness H_d averaged over all stations for all of the 6 months, 4058.26 gpm., and the overall average Γ_d, −1.44° C./km., it becomes

$$H_d = 5486.4 + 20.302\,T_{100},$$

where H_d is in geopotential meters and T_{100} in °C. For a given 100-mb. height H_{100}, a first approximation to the 50-mb. height H_{50} can be obtained, based on the mean overall lapse rate and layer thickness, from

$$H_{50} \approx H_{100} + 20.302\,T_{100} + 5486.4; \qquad (6)$$

this equation (6) was used to construct a nomogram, using H_{100} as ordinate and T_{100} as abscissa, from which the approximate H_{50} could be read off directly. The curves in figure 1 show the correction (gpm.) which must be applied to the nomogram value for latitude (fig. 1A) and for date (fig. 1B) to get the best estimate of the 50-mb. height using Method IV. Since the nomogram itself is a simple linear one it is not shown here.

5. LAPSE-RATE VARIATIONS

The correction curves of figure 1 are also graphs of the

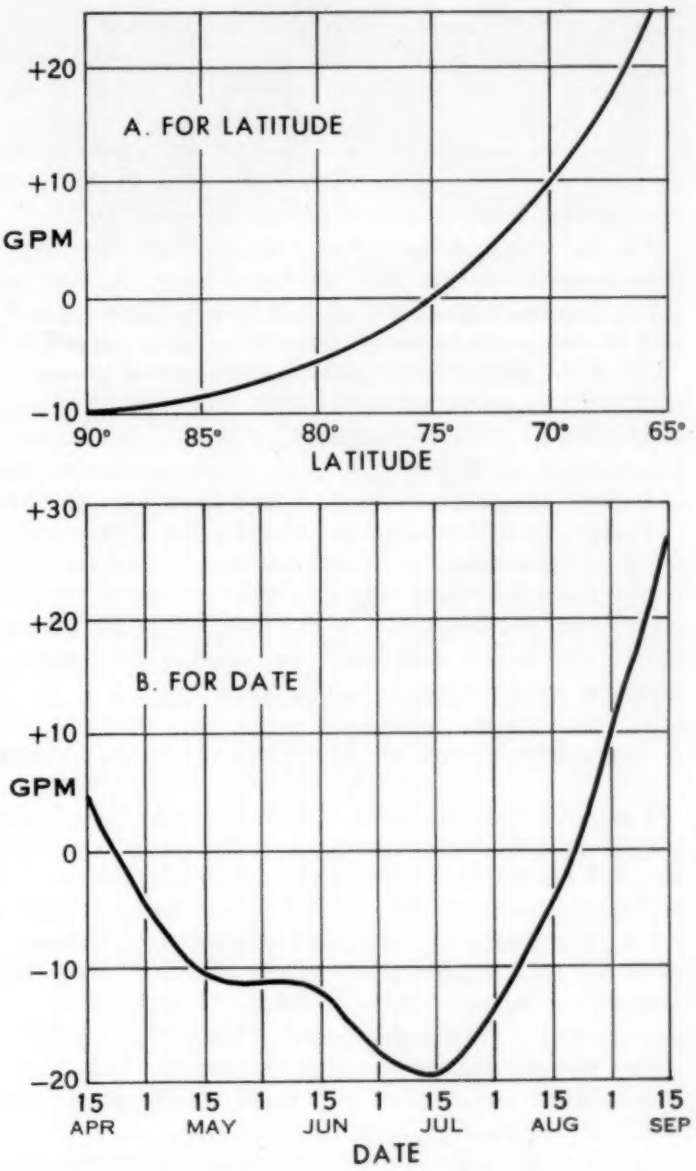

FIGURE 1.—Corrections to extrapolated 50-mb. height: (A) for latitude, (B) for date.

deviations of the layer lapse-rate from the overall mean value of −1.44° C./km., with a correction of 10 gpm. on the ordinate scale the equivalent of a difference in lapse rate of 0.24° C./km. from the mean. Viewed in this light, figure 1A indicates that the stability of the 100 mb. to 50 mb. layer, averaged over the 6 months, April to September, increases in regular fashion from the Pole northward to the Antarctic Circle. Figure 1B shows that in general the layer stability averaged over all latitudes shows a gradual decrease from April until mid-July, and a comparatively rapid increase from then through September.

Comparison with the figures in table 1 shows that while the layer is cooling until mid-July, the stability is decreasing; this means that during this period the 50-mb. temper-

ature is lowering more rapidly than the 100-mb. temperature, as already noted by Wexler [3]. The more rapid cooling at 50 mb. has been explained in terms of the vertical distribution of the atmospheric gases important in long-wave absorption, by Moreland [4], whose investigation indicates a maximum rate of cooling in this layer near 18 km., which is near the 50-mb. winter level.

The flattening of the curve in figure 1B in early June indicates that at this time, the temperature is falling at about the same rate at 100 mb. and 50 mb. Any explanation of this somewhat anomalous behavior is beyond the scope of this paper, although it might be noted in passing that June temperatures during 1957 and 1958 have been anomalous at other atmospheric levels, as demonstrated, for example, in Wexler's [3] study in the section on the "kernlose" Antarctic winter surface temperature pattern.

Finally, it might be well to note that for all of the 6 months, April to September, over the whole range of latitude the temperature falls with height in the 100 mb. to 50 mb. layer, with the exception of the lowest latitude station during the month with most sun (Wilkes, September), when an inversion began in this layer.

6. COMPUTATION OF ADDITIONAL 50-MB. DATA

Table 4 shows the mean observed 50-mb. heights for several months and stations, and the mean computed height of the 50-mb. level from the radiosonde observations terminating between 100 mb. and 50 mb., using Method I for the computations. Method I is chosen here because it gave the best results of any of the four methods when applied to the same stations for which the coefficients were derived. It, therefore, seemed likely that Method I would give the best results when applied not only to the same station but to the very same month which gave the coefficients.

Table 4 also gives the weighted mean of the observed and the computed heights for each month and station for which computations were performed; i.e., those for which data were available and which had a minimum of 8 radiosonde observations reaching 50 mb. Numbers in parentheses following the mean heights are the number of 50-mb. heights, observed or computed, used in determining the mean. The heights are in geopotential meters, with 18,000 gpm. subtracted from each mean to save space.

Observers have noted that sounding balloons in the Antarctic, as elsewhere, tend to reach greater heights when rising through a relatively warm atmosphere than when rising through a relatively cold one. A priori, therefore, one might expect the mean of the computed heights during the Antarctic winter to be lower than that of the corresponding observed heights; however, the results tabulated in table 4 do not demonstrate conclusively any such bias, with the computed means lower than the observed about two-thirds of the time and higher the remaining one-third of the time.

TABLE 4.—*Mean observed and computed 50-mb. heights. Heights in geopotential meters minus 18,000. Parenthetical figures are number of ascents used in determining means. Station-months with fewer than 8 ascents reaching 50 mb. not included*

Station		April	May	June	July	August	September
Pole	Year(s)	----------	1957	1957, 1958	1957, 1958	1957	1957, 1958
	Obs.	----------	908 (30)	640 (61)	388 (34)	308 (10)	324 (29)
	Comp.	----------	952 (17)	627 (48)	264 (68)	313 (37)	289 (48)
	Mean	----------	924 (47)	634 (109)	305 (102)	312 (47)	302 (77)
Byrd	Year(s)	1957	1957	1957	1957	1957	1957
	Obs.	1455 (8)	1004 (20)	859 (29)	448 (24)	416 (27)	457 (17)
	Comp.	1453 (11)	1104 (17)	864 (21)	372 (25)	440 (18)	411 (20)
	Mean	1454 (19)	1050 (37)	861 (50)	411 (49)	426 (45)	432 (37)
Ellsworth	Year(s)	1957, 1958	1958	----------	----------	----------	1957
	Obs.	1569 (52)	1038 (34)	----------	----------	----------	660 (16)
	Comp.	1690 (10)	984 (13)	----------	----------	----------	634 (31)
	Mean	1578 (62)	1023 (47)	----------	----------	----------	643 (47)
Little America V	Year(s)	1957, 1958	1957, 1958	1957, 1958	1957, 1958	1957, 1958	1957, 1958
	Obs.	1661 (71)	1206 (56)	933 (73)	489 (76)	424 (61)	483 (79)
	Comp.	1709 (22)	1374 (34)	942 (18)	455 (31)	416 (28)	431 (25)
	Mean	1672 (93)	1269 (90)	935 (91)	479 (107)	421 (89)	471 (104)
Hallett	Year(s)	1957	1957	1957	----------	1957	1957
	Obs.	1760 (22)	1587 (21)	1138 (13)	----------	656 (32)	899 (25)
	Comp.	1780 (5)	1511 (21)	1106 (18)	----------	569 (19)	900 (24)
	Mean	1764 (27)	1549 (42)	1119 (31)	----------	624 (51)	900 (49)
Wilkes	Year(s)	1957, 1958	1957, 1958	1957, 1958	1957, 1958	1957, 1958	1957, 1958
	Obs.	1957 (71)	1742 (63)	1657 (35)	1030 (38)	850 (35)	958 (57)
	Comp.	1939 (7)	1704 (8)	1642 (13)	942 (50)	797 (47)	933 (29)
	Mean	1956 (78)	1738 (71)	1653 (48)	980 (88)	820 (82)	950 (86)

7. CONCLUSIONS

Before listing conclusions to be drawn from this investigation, it is well to emphasize that only 7 stations' data from two winter seasons were available at the time of writing, and that the stations were concentrated in only about one-half of the continent. The effect of these limiting factors in modifying the conclusions listed is discussed in more detail in the results itemized below.

1. Extrapolated 50-mb. heights obtained using the regression equations with the 100-mb. temperature only as a predictor were as accurate as those obtained from equations using both the 100-mb. height and temperature.

2. Extrapolation of the 50-mb. heights using the assumption of constant lapse rates yields as good results as those of the computed regression equations.

Because of the limited amount of data, conclusions (1) and (2) above should be considered as true only for this set of data. It is entirely possible that the small superiority demonstrated by the constant-lapse-rate method and the single-predictor regression equations is due to chance, and that use of both the 100-mb. height and temperature as predictors might, in a large sample, show improvement over either of the other two methods. It is further possible that addition of different predictors might lead to a further refinement in accuracy; with the limited data it would in any case be impossible to demonstrate that any such improved accuracy was the result of the method's superiority rather than the result of chance, unless the new equations gave 50-mb. heights to a rather unlikely degree of accuracy.

3. The stability of the 100 mb. to 50 mb. layer was, in general, least when the mean temperature of the air was lowest; exceptions were noted in early June, when

the stability remained constant although the mean layer temperature decreased, and in August when some relative warming at 50 mb. increased the stability while the mean temperature was still falling slightly.

4. In the mean, there was a lapse of temperature in the 100 mb. to 50 mb. layer over the portion of the Antarctic considered from April through August, and in September only lower latitudes showed an inversion.

Strictly speaking, conclusions (3) and (4) are valid only for the specific locations and seasons considered. However, these conclusions can probably be extended safely to the continental area in which these stations are concentrated, although extension to the whole Antarctic area would depend on the unsafe assumption of approximate symmetry of temperatures about the geographic pole.

5. From extrapolative methods a considerable amount of additional 50-mb. height data accurate on the average to about 20 gpm. can be obtained for the winter months of the IGY at the Antarctic stations considered.

ACKNOWLEDGMENTS

The writer gratefully acknowledges the encouragement and suggestions received from Dr. Harry Wexler. Thanks are also due to Mr. M. J. Rubin and Mr. S. Teweles for their helpful comments, and to Mr. I. Enger for assistance with some of the statistical methods used. The bulk of the rather onerous computational work was performed by Miss E. E. Marlowe of the Polar Meteorological Research Unit. This work was made possible by support from the National Science Foundation of the National Academy of Sciences, as part of the International Geophysical Year program of the United States.

REFERENCES

1. W. S. Hering and P. Antanaitis, "Specification of the 50-mb. Wind Field by Vertical Extrapolation," *GRD Research Notes* (Contributions to Stratospheric Meteorology), AFCRC–TN–58–450, ASTIA Document No. AD–152626. Geophysics Research Directorate, Air Force Cambridge Research Center, Cambridge, Mass., August 1958.
2. R. J. List (Ed.), *Smithsonian Meteorological Tables*, 6th Revised Edition, Smithsonian Institution, Washington, D.C., 1951 (p. 224)
3. H. Wexler, "Seasonal and Other Temperature Changes in the Antarctic Atmosphere," *Quarterly Journal of the Royal Meteorological Society*, vol. 85, No. 365, July 1959, pp. 196–208. Also (in Russian) in *Meteorologiia i Gidrologiia*, Leningrad, No. 3, March 1959, pp. 10–24.
4. W. B. Moreland, "Antarctic Stratospheric Thermal Structure, Circulation and Ozone Observations," paper delivered at *Symposium* on Antarctic Meteorology, Melbourne, Australia, February, 1959. (To be published.)

Recent Articles in Other Weather Bureau Periodicals

Weekly Weather and Crop Bulletin, National Summary, vol. XLVII:
No. 24, June 13, 1960
"Climatological Summaries for the Smaller Communities" by J. R. Swartz
No. 33, Aug. 15, 1960
"Weather and Forest Fires" by L. M. LaMois

Mariners Weather Log, vol. 4:
No. 4, July 1960
"The Hurricane Voyage of the Yacht *Esprit*" by J. B. Cox, pp. 99–101
"Hurricane Tracking at Sea" by G. B. Clark, pp. 102–103
No. 5, September 1960
"Some Aspects of the Wind Field in Hurricanes" by J. A. Colón, pp. 145–150.
"SS *DeSoto* Encounters Hail Storm in Gulf of Mexico" by D. L. Olson, pp. 150–151.
"Synoptic Analysis of Hail Storm Encountered by SS *DeSoto*, April 2, 1960" by W. A. Hass, pp. 151–153.

Weather Note

RAPID PRESSURE VARIATIONS IN ICELAND

EYSTEINN TRYGGVASON

Geophysical Section, Vedurstofa Islands, Reykjavik, Iceland

[Manuscript received June 27, 1960]

In the "Weather Note", *Monthly Weather Review*, January 1960 an unusual pressure rise at Yakutat is described [1]. As the note asked for information about similar or larger pressure rises, I want to give a brief description of an unusual cyclone with rapid pressure variations that struck the east coast of Iceland on January 25, 1949. This cyclone had a central pressure of about 940 mb., its radius was approximately 200 km., and it moved with a velocity of about 70 km./hr., N. 15° E.

The most rapid pressure variations occurred at Dalatangi, where the following pressure observations were made:

	Sea level pressure
January 25, 0900 GMT	977.8 mb.
1200	973.7
1500	963.0
1800	952.5
2100	975.6
2400	981.7

According to the barograph trace at the station (fig. 1), the lowest pressure, 941 mb., occurred at 1715 GMT. The maximum pressure fall in 1 hour was from 956 mb. at 1600 GMT to 942 mb. at 1700 GMT, or 14 mb. The maximum fall in 3 hours was 26 mb. The maximum pressure rise in 1 hour was from 941.5 mb. at 1740 GMT to 960.5 mb. at 1840 GMT, or 19 mb. The maximum pressure rise in 3 hours was 33 mb.

The barograph trace made at Hôlar, Southeast Iceland, was very similar to that at Dalatangi with minimum pressure of 947 mb. and maximum pressure rise of 18 mb. in 1 hour.

Pressure rises of similar magnitude as that described in [1] have been observed several times at Icelandic weather stations. Three examples observed in Reykjavik during the last 12 years are:

	1-hour pressure rise	3-hour pressure rise
January 22, 1950	12 mb.	20 mb.
January 5, 1952	7	18
March 8, 1953	9	19

REFERENCE

1. Mac A. Emerson, "Pressure Rise at Yakutat, December 18, 1959," Weather Note, *Monthly Weather Review*, vol. 88, No. 1, January 1960, p. 18.

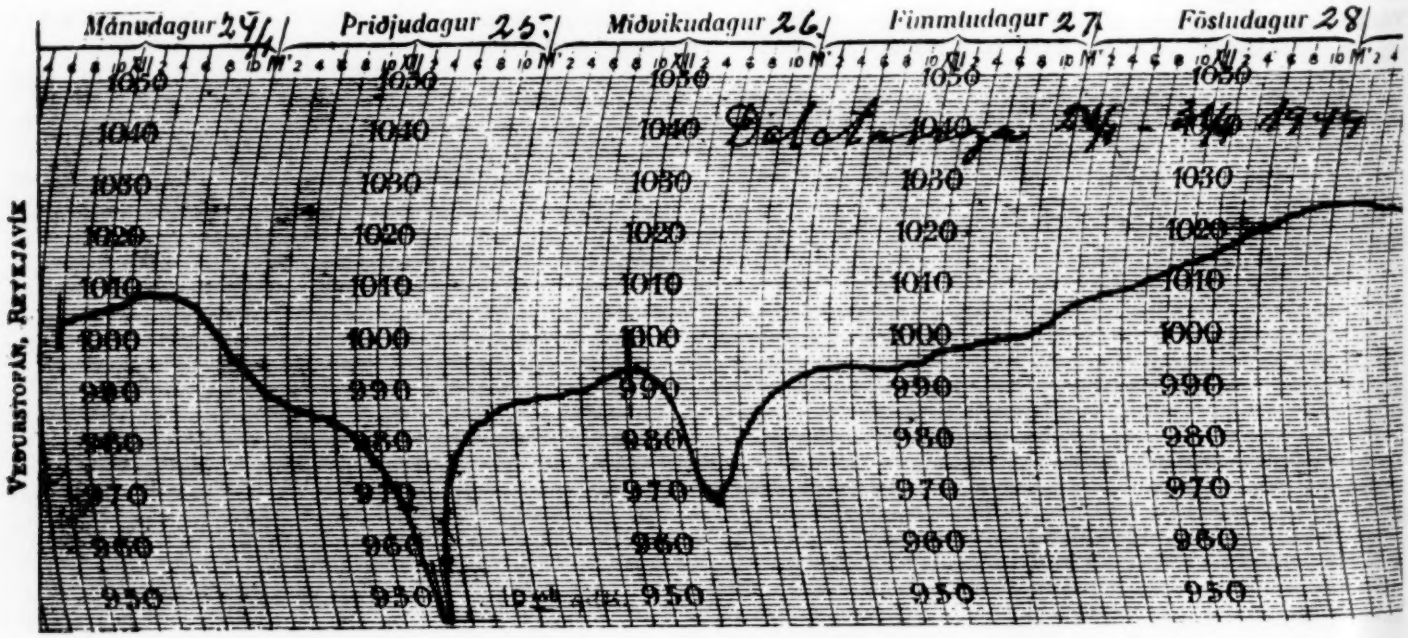

FIGURE 1.—Photocopy of section of barograph trace made at Dalatangi, Iceland, January 24–31, 1949.

THE WEATHER AND CIRCULATION OF JULY 1960

Persistent Heat in the Pacific Northwest

RAYMOND A. GREEN

Extended Forecast Section, U.S. Weather Bureau, Washington, D.C.

1. HIGHLIGHTS

July 1960 was especially noteworthy for prolonged, excessive heat in the Pacific Northwest. The greatest departures of average temperature from normal, more than 6° F., were centered on the Oregon-Idaho boundary (fig. 1). New temperature records at Boise, Idaho included an all-time high of 111° F. on the 19th, 27 days with 90° or higher, 11 days with 100° or higher, and the highest monthly average in 62 years. New records at other stations appear in table 1. Sustained high temperatures, low humidity, and little precipitation brought, in the words of LaMois of the U.S. Forest Service [1] ". . . extremely critical burning conditions throughout the Western States during July. More than 4,000 fires occurred, most of which started from heavy concentrations of lightning storms which struck California, Oregon, Washington, Montana, and Idaho . . . . The fire fighting bill during July alone was more than $15 million."

Abnormal warmth over the western half of the United States was accompanied by unseasonable coolness over much of the eastern half, with greatest departures in a band from northern Texas to eastern Pennsylvania (fig. 1). New low averages for July were also numerous. Cleveland, Ohio headed the list (table 1) with an average temperature of 67.6° F. and a departure from normal of −6.1° F.

TABLE 1.—*New record average temperatures for July, and their departures from normal, observed in 1960*

	Monthly average (° F.)	Departure from normal (° F.)
	High temperature	
Boise, Idaho	80.7	+5.9
Nome, Alaska	54.3	+4.7
Salt Lake City, Utah	81.2	+4.6
Pendleton, Oreg	78.3	+3.8
Idaho Falls, Idaho	71.8	+2.6
Miami, Fla	83.7	+1.1
	Low temperature	
Cleveland, Ohio	67.6	−6.1
Youngstown, Ohio	67.9	−3.7
Pittsburgh, Pa	68.6	−3.7
Philadelphia, Pa	*73.2	−3.1
Wilmington, Del	**73.1	−2.8

*Equaled in 1895.
**Equaled in 1894.

Tropical storm Brenda moved up the east coast the last few days of the month. It caused little wind damage, but heavy rains were reported along its path.

2. MEAN CIRCULATION

From June to July high-latitude blocking diminished over northern Canada and increased over the Siberian Peninsula (+260 feet, fig. 2). During July two 5-day mean blocking ridges coalesced with the subtropical ridge in the Pacific, and amplification of the circulation occurred downstream at middle latitudes. Height anomalies in the troughs and ridges of figure 2 were generally larger than their June counterparts, and a new mean wave was introduced into the pattern in the eastern Atlantic. Further evidence of large amplitudes in July is given by the displacement of the principal axis of maximum mean 700-mb. winds. In figure 3 it can be seen that in mean troughs of the western part of the hemisphere southward displacement of the "jet stream" occurred, while in the ridges the displacement was northward except in the central Pacific.

The slow-down of the temperate westerlies was not as great as one expects to observe with amplification of this magnitude. A drop of only 0.2 m.p.s. from the preceding

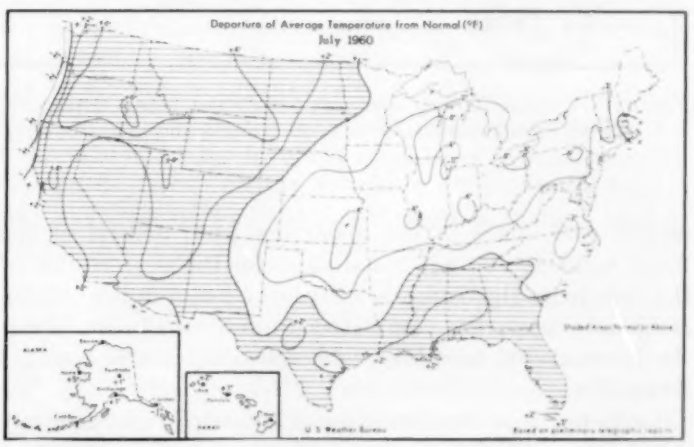

FIGURE 1.—Departure of average temperature from normal (°F.) for July 1960. Noteworthy features include abnormal warmth in the Northwest and coolness from the Central Plains northeastward. (From [2].)

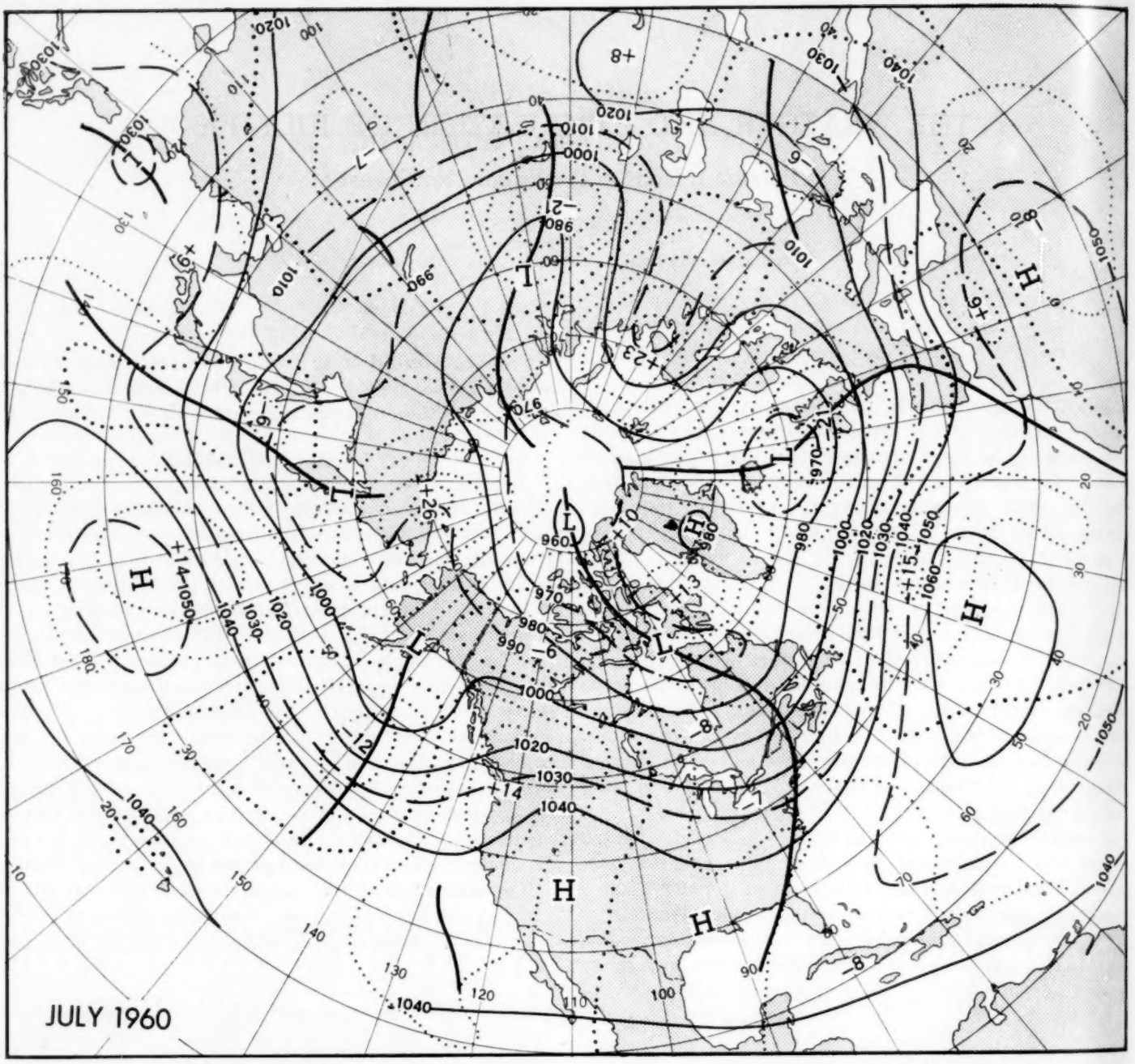

FIGURE 2.—Mean 700-mb. contours (solid) and height departures from normal (dotted), both in tens of feet, for July 1960. Greater than normal amplitude of mean troughs and ridges in temperate latitudes is suggested by departure from normal pattern.

month took place in the departure from normal of the mean monthly 700-mb. zonal index for the western half of the Northern Hemisphere. Five-day mean indices of the temperate westerlies completed a minor oscillation about the normal by mid-July and remained above normal thereafter.

Large negative changes of mean 700-mb. height anomaly from June to July, shown in figure 4, indicated strong deepening over the eastern Pacific and the British Isles at temperate latitudes, while falls over northern Canada and rises over the Asian sector of the Arctic Basin attended the migration of blocking at high latitudes. Over western Canada, rises reflected the growth of the mean ridge which strongly influenced the temperature pattern of the United States.

3. TEMPERATURE

The mean ridge at 700 mb. over the Pacific Northwest was both stronger than normal and persistent. Five-day mean height anomalies there remained well above normal the entire month. Not once did the weekly average temperature fall below normal at reporting stations in Idaho

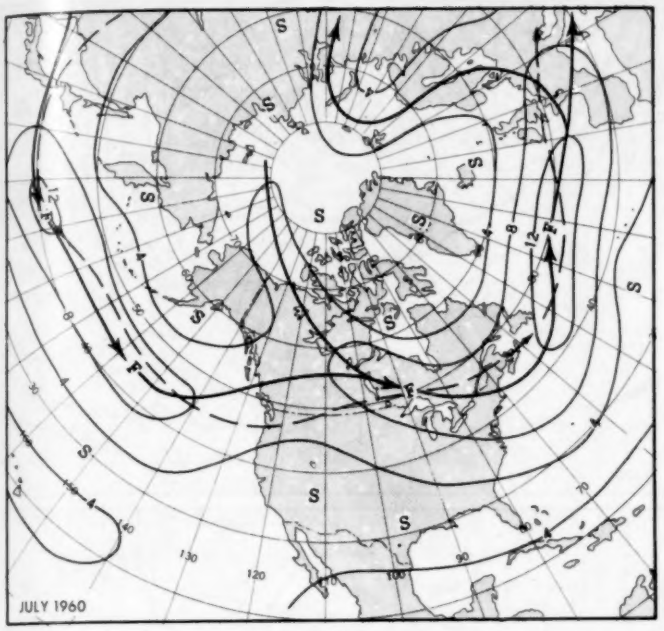

FIGURE 3.—Mean 700-mb. isotachs (in meters per second) for July 1960. Solid arrows indicate axes of west wind maxima, dashed arrows the normal for the month. Eastward from the central Pacific the primary axis was displaced southward from normal in mean troughs and northward from normal in ridges.

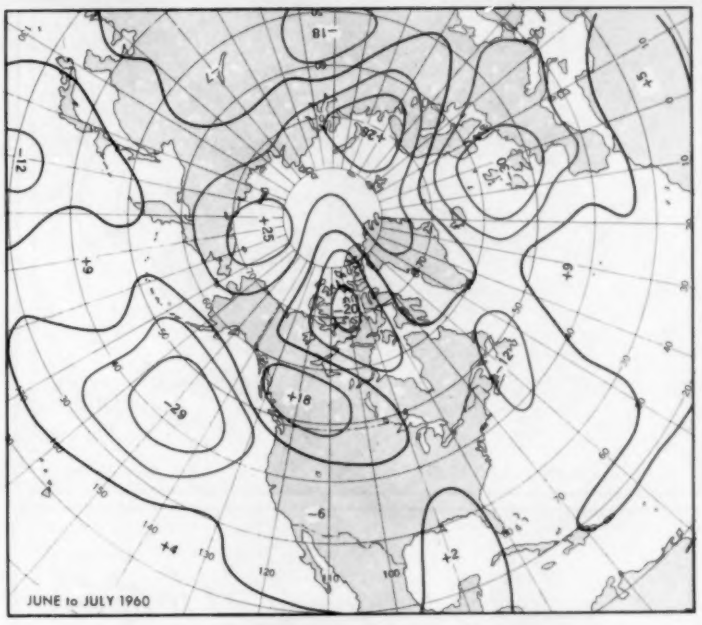

FIGURE 4.—Difference between monthly mean 700-mb. height anomaly for June and July 1960 (July minus June) in tens of feet. Pronounced deepening occurred in the northeastern sections of the Pacific and the Atlantic. Large changes at polar latitudes accompanied the migration of blocking from northern Canada.

and inland sections of Oregon and Washington [2], and the same was true in Montana after the week ending July 3. Thus the extent and intensity of warm temperature anomalies were largely products of persistence.

One locally effective warming factor was the downslope flow indicated by the departures from normal of mean 700-mb. height in figure 2. The flow was generally northeasterly where centers of maximum departure were observed in valleys of Idaho, Utah, and California which lie southwestward from extensive mountain barriers. Perhaps of greater importance was the fact that more than 80 percent of possible sunshine was realized at most stations in the anticyclonic environment of the Northwest.

Over the remainder of the Nation there was more intramonthly variability of the anomalies of both temperature and 700-mb. height. Even so, temperatures averaged at least slightly less than normal each week in Pennsylvania and sections of Ohio and New York adjacent to Lakes Erie and Ontario. Scattered stations westward as far as the Central Plains also reported subnormal averages for every week of the month [2].

Most of July's area of below-normal temperature was also in the below category in the mean patterns for spring and for June [3]. Exceptions were a semicircular region from southeastern Colorado to central Texas and Atlantic Coastal States northward from Virginia. In general the cool temperatures of July were what might be anticipated from the mean height anomaly field and the cyclonic northwesterly flow in figure 2. In addition, the large amplitude of the mean circulation supported a southward displacement from normal of the tracks of daily Highs and Lows (fig. 5). One branch of the paths of both dipped abnormally far into the United States, augmenting the southward penetration of cool Canadian air.

Cooling over the Soushwest from the extreme heat of June left that section of the country only slightly above normal in July. A similar change took place in the Northeast. Changes of the temperature anomalies from June to July followed rather closely the changes of 700-mb. height anomaly in figure 4. Thus general cooling occurred along a diagonal band oriented southwest to northeast, and general warming over the Northwest and the Southeast. Among 100 selected stations the largest change was only 2 classes, qualitatively indicative of more than usual month-to-month persistence. This is quantitatively verified by the fact that 76 of the stations appeared in the 0- or 1-class change category, while Namias found June to July persistence of these classes 72 percent on the average from 1942 to 1954 [4].

4. TROPICAL STORM BRENDA AND PRECIPITATION

Brenda formed in the eastern Gulf of Mexico in late July. The behavior of the mean circulation prior to and during the storm's short life is depicted in the series of overlapping 5-day mean 700-mb. maps in figure 6. On the chart for July 21–25 (A) a deep mean trough extended along the Atlantic coast well into the Tropics from Labrador. By July 23–27 (B) the trough had sheared, and

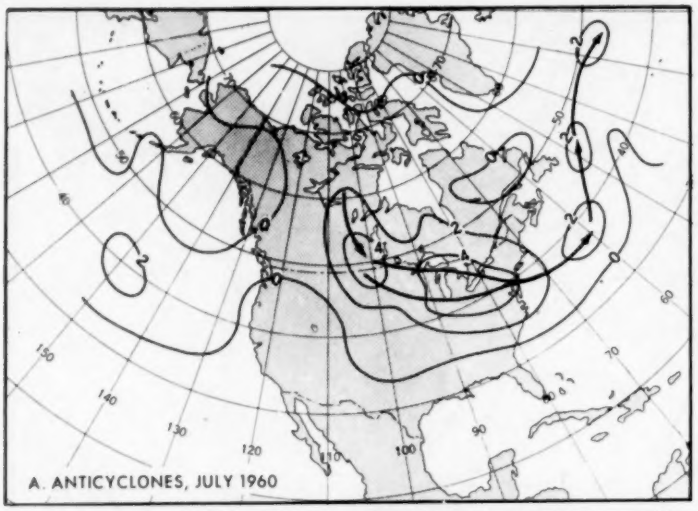

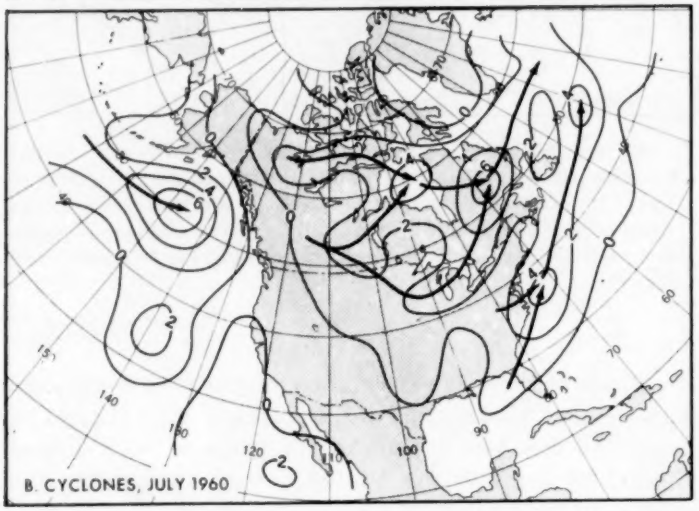

FIGURE 5.—Number of (A) anticyclone passages and (B) cyclone passages within quadrilaterals of 66,000 square nautical miles during July 1960. Primary tracks are indicated by solid arrows. Branches of the tracks of both anticyclones and cyclones pushed abnormally far southward into United States. Note the scarcity of migrating systems west of the Continental Divide.

the tropical portion retrograded to Florida, while the northern portion of a similarly sheared trough advanced from Oklahoma to Indiana. By July 26–30 (C) the fractured parts of the troughs were joined with the Hudson Bay Low to form a deep mean trough across the Great Lakes and the eastern Gulf of Mexico. Brenda formed in this trough.

The subsequent path of the storm coincided rather closely with the 30-day mean trough line of figure 2. This tendency for storms to move along mean troughs has been discussed by Klein [5], who listed numerous examples from previous years. With such coincidence the question of cause and effect often arises, since it may be argued that low pressures in the storm largely determine the location of the trough. For example, see the

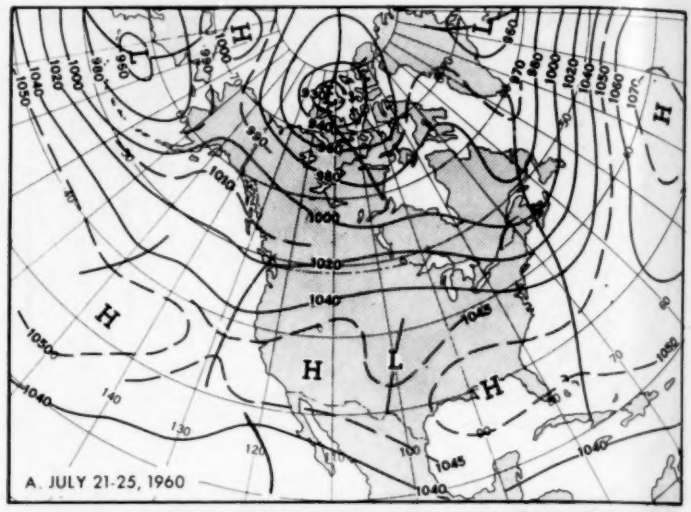

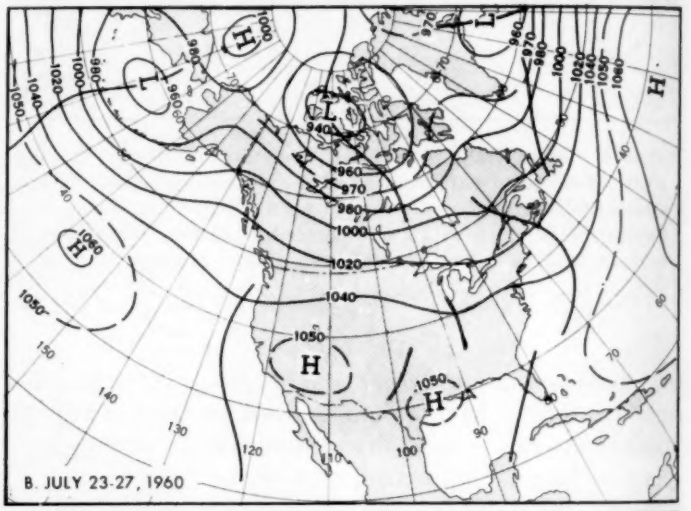

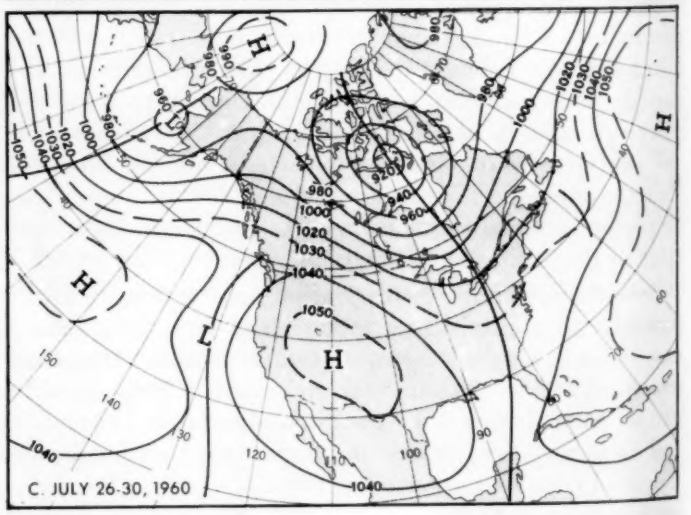

FIGURE 6.—Five-day mean 700-mb. contours in tens of feet for (A) July 21–25, (B) July 23–27, and (C) July 26–30, 1960. Tropical portion of mean trough in the western Atlantic (A) retrograded to Florida (B) and joined with sheared portion over western Indiana to form deep trough through eastern Gulf of Mexico (C) where tropical storm Brenda developed. Heavy rains occurred on July 23 and 24 near the mean Low over Oklahoma (see A).

TABLE 2.—*Selected precipitation totals (inches) for July including totals during close proximity of Brenda*

	Total for July	Total during Brenda
Tampa, Fla.	*20.59	16.36
Orlando, Fla.	*19.57	10.79
Jacksonville, Fla.	*16.21	1.57
Savannah, Ga.	*15.70	2.89
Ft. Myers, Fla.	13.76	4.42
Charlestott, S.C.	11.74	4.43
New York, N.Y.	*9.97	4.90
Bridgeport, Conn.	8.13	3.57
Richmond, Va.	7.34	2.39
Wilmington, Del.	6.18	2.51

*New record for July.

correspondence between Ramage and Ballenzweig in a recent issue of the *Journal of Meteorology* [6]. To throw some light on this question, a mean map of the 25 July days preceding Brenda was constructed (fig. 7). The storm path superimposed on this pattern follows the mean trough line rather well. Obviously in this case the low pressures of the storm altered the mean 30-day trough position very little.

The storm's effect on the precipitation pattern (fig. 8), however, was more substantial. Rainfall totals from Brenda comprised a large proportion of the monthly amount at a number of stations, as revealed by table 2, where both totals are tabulated for comparison. At Tampa, Fla., more than three-fourths of the monthly accumulation could be attributed to the storm. In general, much higher proportions of the monthly amounts were caused by the storm near the area of its formation than elsewhere along the path where rapid motion occurred. During Brenda's passage new records for 24-hour rainfall were established at Orlando and Tampa, Fla., and at New York City.

Most of the precipitation in the Great Lakes Region is attributable to frontal Lows traversing the southward displaced storm track of figure 5B. An additional feature of interest associated with the first of these Lows was the outbreak of tornadoes in North Dakota on July 2 and in Indiana on the 3d. Other tornadoes were reported later in the month, mostly after the 20th, and were most frequent from the Southern Plains to Iowa. Only those in Iowa were clearly associated with frontal troughs, while the remainder occurred beneath cyclonic upper flow in maritime tropical air.

Rainfall was more than twice the normal from the Texas Panhandle to Arkansas, where moisture was in adequate supply in the weak flow from the Gulf of Mexico around the mean High centered over eastern Texas (fig. 2). Some of this precipitation was frontal in nature, but the heaviest, in eastern Oklahoma and western Arkansas, was triggered by a trough which formed during a readjustment of mean waves. When the wavelength downstream from the retrograding Pacific trough became long, new mean troughs appeared on the 5-day mean map for July 19–23 (not shown) along the west coast and over Oklahoma. Both are shown in the mean circulation of figure 6A for

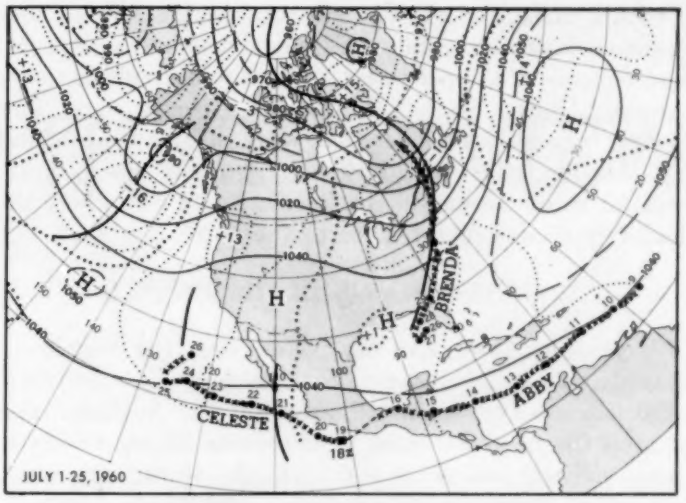

FIGURE 7.—Mean 700-mb. contours (solid) and height departures from normal (dotted), both in tens of feet for July 1–25, 1960. This represents the mean circulation prior to the formation of tropical storm Brenda (dotted track, east coast) which traveled up the mean trough (heavy vertical line). Also depicted are paths of hurricanes Abby and Celeste. Large dots indicate 1200 GMT positions of storms, and numbers the July date of each position.

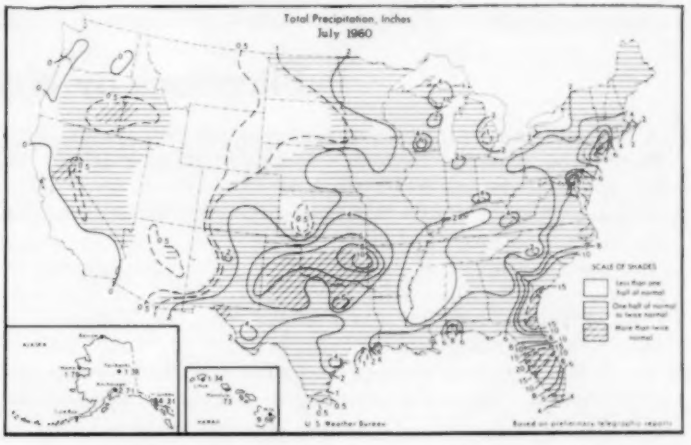

FIGURE 8.—Total precipitation (inches) for July 1960. Record monthly amounts for July were observed along the east coast. (From [2].)

July 21–25. The Oklahoma trough was the stronger of the two, and heavy rain occurred in its vicinity during the 23d and 24th. Subsequently a portion of this trough advanced to join the mean trough in which Brenda was spawned, while the trough near the west coast strengthened and advanced enough to bring showers and local temporary relief from critical burning conditions in forested areas of the Far West.

Practically no rain had fallen over the western tier of States until this time. Dry weather also prevailed over adjoining States and from Montana to Arizona (see fig. 8), where the general accumulation was less than half an inch. Sheridan, Wyo., had 3.51 inches during the period from January to July, the driest like period ever recorded; and

Phoenix, Ariz., reported no measurable rain for 143 consecutive days ending July 23. The dryness was a natural consequence of the persistent anticyclonic circulation over western United States. Migratory cyclones were completely absent from the area west of the Continental Divide (fig. 5B). In addition, orographic precipitation was far below normal in the Pacific Northwest where the mean "jet" was diverted far to the north (fig. 3).

5. OTHER STORMS IN THE TROPICS

Hurricane Abby was discovered near the Windward Islands. It reached hurricane intensity on the 10th, traveled steadily westward near 15° N. latitude, and skirted the northern coast of Honduras during the 14th. After moving inland on the 15th, the storm apparently dissipated and dropped from sight. On the basis of continuity, however, it is likely that remnants of the storm were instrumental in the formation of hurricane Celeste on the 19th (see dashed continuation of Abby, fig. 7). Celeste moved west-northwestward well off the coast of Mexico, turned westward south of Baja California, on the 22d, weakened to a tropical storm the following day, and dissipated thereafter.

In the western Pacific two storms attained typhoon intensity. Typhoon Polly formed east of Luzon, P.I., on July 19 and took a slow northerly track through the East China Sea and the Yellow Sea, reaching the coast of Manchuria on the 29th. Shirley also formed east of the Philippines, but took a more westerly course and struck Formosa on the last day of the month.

REFERENCES

1. L. M. LaMois, "Weather and Forest Fires," *Weekly Weather and Crop Bulletin, National Summary*, vol. XLVII, No. 33, August 15, 1960, p. 7.
2. U.S. Weather Bureau, *Weekly Weather and Crop Bulletin, National Summary*, vol. XLVII, Nos. 27–31, July 4, 11, 18, 24, August 1, 1960.
3. C. M. Woffinden, "The Weather and Circulation of June, 1960—A Hot Dry Month in the Southwest," *Monthly Weather Review*, vol. 88, No. 6, June 1960, pp. 229–234.
4. J. Namias, "The Annual Course of Month-to-Month Persistence in Climatic Anomalies," *Bulletin of the American Meteorological Society*, vol. 33, No. 7, Sept. 1952, pp. 279–285 (and an unpublished extension through 1954).
5. W. H. Klein, "The Weather and Circulation of June 1957—Including an Analysis of Hurricane Audrey in Relation to the Mean Circulation," *Monthly Weather Review*, vol. 85, No. 6, June 1957, pp. 208–220.
6. C. S. Ramage, "Long-Period Circulation Anomalies and Tropical Storms," *Journal of Meteorology*, vol. 17, No. 3, June 1960, p. 375, and Reply by E. M. Ballenzweig, pp. 375–376.

Publications by Weather Bureau Authors

J. K. Angell, "An Analysis of Operational 300 Mb. Transosonde Flights from Japan in 1957–58," *Journal of Meteorology*, vol. 17, No. 1, Feb. 1960, pp. 20–35.

K. Butson, "Florida Winter Weather: 1957–58," *Weatherwise*, vol. 11, No. 2, Apr. 1958, pp. 58–59.

N. L. Canfield, "Review of *Atlas of 300-mb. Wind Characteristics for the Northern Hemisphere*, by Lahey et al., Univ. of Wisconsin Press, Madison, 1960," *Bulletin of the American Meteorological Society*, vol. 41, No. 7, July 1960, p. 399.

C. B. Carney, "Freeze Damage to Plants," *Weekly Weather and Crop Bulletin, National Summary*, vol. XLVI, No. 21, May 25, 1959, pp. 7–8.

G. P. Cressman, "Hemispheric Nondivergent Barotropic Forecasting," *The Atmosphere and the Sea in Motion*, Scientific Contributions to the Rossby Memorial Volume, Bert Bolin, Ed., The Rockefeller Institute Press in association with Oxford University Press, New York, 1959, pp. 475–485.

R. A. Dightman, "An Application of Climatology to Alfalfa Harvesting," *Weekly Weather and Crop Bulletin, National Summary*, vol. XLVI, No. 28, July 13, 1959, p. 8.

S. Fritz, "Satellite Meteorology," in "United States National Report 1957–1960 Twelfth General Assembly, International Union of Geodesy and Geophysics," *Transactions of the American Geophysical Union*, vol. 41, No. 2, June 1960, pp. 217–220.

J. G. Georg, "Cranberry Crop and Weather in Wisconsin, 1959," *Weekly Weather and Crop Bulletin, National Summary*, vol. XLVI, No. 41, Oct. 12, 1959, pp. 7–8.

D. L. Harris, "Storm Surges," in "United States National Report 1957–1960, Twelfth General Assembly International Union of Geodesy and Geophysics," *Transactions of the American Geophysical Union*, vol. 41, No. 2, June 1960, pp. 266–269.

H. E. Landsberg, "Do Tropical Storms Play a Role in the Water Balance of the Northern Hemisphere?" *Journal of Geophysical Research*, vol. 41, No. 4, Apr. 1960, pp. 1305–1307.

H. E. Landsberg, "Review of *General Climatology*, by H. J. Critchfield, Prentice-Hall, Englewood Cliffs, N.J., 1960," *Science*, vol. 131, No. 3417, 24 June 1960, p. 1882.

A. R. Long, "Dry Weather in Alabama, October 1958–August 1959," *Weekly Weather and Crop Bulletin, National Summary*, vol. XLVI, No. 35, Aug. 31, 1959, p. 8.

L. Machta, "Meteorological Factors and Fallout Distribution," pp. 33–56 in *Low-Level Irradiation*, Austin M. Brues, Editor, Publication No. 59 of the American Association for the Advancement of Science, Washington, D.C., 1959, 148 pp.

L. Machta and R. J. List, "The Global Pattern of Fallout," Chapter 2 (pp. 26–36) in *Fallout, A Study of Superbombs, Strontium 90 and Survival*, John M. Fowler, ed., Basic Books, Inc., New York, 1960, 235 pp.

F. Ostapoff, "Antarctic Oceanography" in "United States National Report, 1957–1960, Twelfth General Assembly International Union of Geodesy and Geophysics," *Transactions American Geophysical Union*, vol. 41, No. 2, June 1960, pp. 257–258.

J. C. Purvis, "Weather and Peaches in South Carolina," *Weekly Weather and Crop Bulletin, National Summary*, vol. XLVI, No. 2, Jan. 12, 1959, pp. 6–8.

A. D. Robb, "Rose Culture and the Weather," *Weekly Weather and Crop Bulletin, National Summary*, vol. XLVII, No. 2, Jan. 11, 1960, p. 8.

L. H. Seamon, "Weather of the Year 1958," *Weekly Weather and Crop Bulletin, National Summary*, vol. XLVI, No. 4, Jan. 26, 1959, pp. 7–8.

S. Teweles and F. G. Finger, "Reduction of Diurnal Variation in the Reported Temperatures and Heights of Stratospheric Constant-Pressure Surfaces," *Journal of Meteorology*, vol. 17, No. 2, Apr. 1960, pp. 177–194.

H. Wexler, "Satellites et Meteorologie," *Met-Mar*, Bulletin Trimestriel de Liason et d'Information, No. 28, Direction de la Meteorologie Nationale, Paris, April 1960, pp. 13–19.

U.S. GOVERNMENT PRINTING OFFICE: 1960